energies

MDPI

Article

Powers and Power Factor in Non-Sinusoidal and Non-Symmetrical Regimes in Three-Phase Systems

Petre-Marian Nicolae [1,*], Ileana-Diana Nicolae [2] and Marian-Ştefan Nicolae [1]

[1] Faculty of Electrical Engineering, University of Craiova (UCV), 200440 Craiova, Romania; stefan.nicolae@edu.ucv.ro
[2] Faculty of Automatics, Computer Science and Electronics, University of Craiova (UCV), 200440 Craiova, Romania; ileana.nicolae@edu.ucv.ro
* Correspondence: petre.nicolae@edu.ucv.ro

Abstract: The paper presents several theories related to definitions of powers and power factors in non-sinusoidal and non-symmetrical regimes. The theories must meet some requirements: (a) to facilitate the measuring of power quantities by using acquired electrical waveforms; (b) to support the correct quantification of powers and power factors for a fair charge; (c) to support solutions for efficient compensation of non-sinusoidal and non-symmetrical regimes, simultaneous with the power factor compensation along the fundamental harmonic. Only theories meeting the above-mentioned requirements are approached. Aspects specific to power definitions are discussed and commented. Three theories rely on the Fourier decomposition of non-sinusoidal waveforms, valid only for steady signals, whilst the fourth relies on the Discrete Wavelet Transform (DWT) and can also be applied to unsteady signals. Dedicated original data acquisition systems were used to acquire experimental data for three case studies. Data were analysed with original software tools, based on the Fast Fourier Transform and Discrete Wavelet Transform, implementing the approached theories. Comparisons between results yielded for analogue quantities proved that the approached theories satisfy the requirements for which they were created, except for the fourth theory, which can be used only for compensation purposes.

Keywords: powers theories; power factor; active; reactive; distorting; apparent and non-active powers; dedicated data acquisition systems; Fast Fourier Transform; Discrete Wavelet Transform

check for updates

Citation: Nicolae, P.-M.; Nicolae, I.-D.; Nicolae, M.-Ş. Powers and Power Factor in Non-Sinusoidal and Non-Symmetrical Regimes in Three-Phase Systems. *Energies* **2022**, *15*, 5130. https://doi.org/10.3390/en15145130

Academic Editor: Tek Tjing Lie

Received: 27 May 2022
Accepted: 12 July 2022
Published: 14 July 2022

Publisher's Note: MDPI stays neutral with regard to jurisdictional claims in published maps and institutional affiliations.

Copyright: © 2022 by the authors. Licensee MDPI, Basel, Switzerland. This article is an open access article distributed under the terms and conditions of the Creative Commons Attribution (CC BY) license (https://creativecommons.org/licenses/by/4.0/).

1. Introduction

In 1927, the Romanian Academician Constantin Budeanu published the book "Puissances reactives et fictives", providing the first evaluation of powers in a mono-phase system. He noticed the need for defining an additional power (distorting power) apart from the traditional active, reactive and apparent powers. This new power, along with the active and reactive powers, was intended to provide a correct power balance [1]. For this aim, he used decompositions in the Fourier series of the non-sinusoidal periodic quantities and defined the power balance through an analogy with the sinusoidal regime by using the squares of the quantities. The power electronics and power systems did not have present popularity at that time and, therefore, C. Budeanu addressed only the mono-phase systems. In the same period, other formulations addressing powers in mono-phase systems were issued, mainly in Europe (Romanian, Polish, Italian, German). They had particular points of view and developed different concepts.

Later, with the development of energy systems and the need to find a balance between production and consumption from a technical point of view, but also for the needs of measurement and taxation, several theories were developed for three-phase systems. Each proposed the separation of powers into components considering various points of view [2–6]. But each of them must meet certain requirements in order to be accepted as theories of power for three-phase systems. First of all, such a theory must offer the possibility of measuring the power components for three-phase situations. Second, it must provide effective real-time compensation solutions. Thirdly, it must offer the possibility to analyse the proposed solutions after compensation, both from a technical point of view and from a financial point of view—related to the return of the investment (ROI) addressed to those who take compensation actions.

Initially, all the developed theories were based on the Fourier series decompositions of non-sinusoidal periodic waveforms of currents and voltages for steady signals.

Over time, due to the theoretical development toward the infinity of harmonic orders, it was necessary to limit them to allow the calculation of power components and power/energy quality indices.

Therefore, standards were issued. They limited the harmonic components, settling decomposition into a number of harmonics up to the 40th order according to European standards (e.g., EN 50160 [7]) or up to the harmonic ordinal 50—according to IEEE standards (e.g., IEEE Standard 519—2010 [8]).

The proposed limits had to consider particular technical and computational aspects. For example, industrial data acquisition systems used to acquire data for waveforms from three-phase systems simultaneously can offer a sampling rate lower than that used for mono-phase quantities. This represents a limitation for the maximum harmonic order, which can be computed (e.g., electromagnetic interferences cannot be estimated) and this can result in unacceptable computational errors. On the other hand, commercial software tools do not always use and usually cannot suggest the correct number of points to be used for discretization, such as to get the necessary accuracy of yielded results in different operational contexts.

Some theories rely only on the decomposition of three-phase currents into components defined by authors (e.g., "Currents' Physical Components (CPC) power theory" [9,10]). They do not provide an exhaustive image of the power quantities, mainly on the consumer's side, where both voltages and currents have non-sinusoidal waveforms.

Such definitions can only be useful to power suppliers for medium or high voltage levels, where the voltages are almost sinusoidal.

Actually, such operational contexts are speculated by the power suppliers with respect to power definitions. They measure the powers/energies of consumers in test points with medium/high voltages and charge the consumers according to the measurement results. Moreover, the power suppliers include in the power price the losses from their transformers used to supply power to consumers (CT) by measurements conducted in test points with medium or high voltage, placed in front of the primary winding of the CTs. As long as the secondary winding of such CT can be used to supply more consumers, this scenario can also involve an unresolved legal issue, which can be used as an advantage by power suppliers.

Considering the above, one can say that the definitions of the powers in three-phase systems should consider both voltages and currents as being quantities with non-sinusoidal variations to provide usefulness for the given definitions and offer solutions to the previously detected problems.

Certain theories can act in a limited number of directions (e.g., for the load compensation while being unable to provide relevant solutions for measurement and charging [11–13]).

Problems related to the non-symmetrical regimes should be considered along with those related to non-sinusoidal regimes. Such regimes can be caused either by non-symmetries in the supplying voltages or by the unbalance of consumer(s). In the first case, the solution may be solved at the supplying sources and consists of voltages symmetrisation. For the second case, usually, one has to make schematics to balance the consumers (e.g., the Steinmetz Connection). The presence of nonlinear loads can also lead to a combination of non-symmetrical and non-sinusoidal regimes. As a consequence, in such situations, many conclusions related to powers should take into account decompositions of periodic quantities by using the Fourier series while providing the ability to separate the voltage/current components into harmonic components that follow certain sequences (+, −, or 0).

This paper presents some of these theories, along with the authors' points of view. Three of them rely on Fourier decompositions and can be applied only at (quasi)steady waveforms, whilst the fourth relies on the Discrete Wavelet Transform (DWT) which is applicable without such restrictions.

Recent progress in data acquisition systems and dedicated software tools made possible the re-evaluation of certain theories, opening the road for a unitary approach with regard to the possibilities of measurement, charging and compensation and maybe future joint utilization with other theories.

A fourth theory addresses the possibility of performing compensation measures in (quasi)steady regimes based on active or hybrid filtering. However, considering its theoretical aspects, it allows relevant alternatives neither for the measuring of the entire spectrum of powers nor for solutions of correct charging.

Some examples of theories applied in cases of significantly distorted regimes are provided to justify the use of a certain theory, along with comments.

2. Theories of Powers in Three-Phase Systems Operating in Non-Sinusoidal and Non-Symmetrical Regimes

Several theories which try to define different categories of powers are non-sinusoidal and non-symmetrical operating regimes of three-phase circuits/networks were conceived along time. Four of them are addressed in this paper. Three of them rely on the decomposition of non-sinusoidal voltages and current waveforms with the Fourier transform. According to different standards for quality of energy/power, the number of harmonic orders used during decomposition can be different: 40—according to the standard EN 50160 or 50—according to the standard IEEE 519—2010. On the other hand, it is the particular topology of the decomposition tree used by DWT that imposes the maximum harmonic order (e.g., it is 256 for a root node hosting 512 components and seven levels, using a wavelet mother of type Daubechies with a filter of length 28).

2.1. The Theory Relying on Powers Decomposition into Active, Reactive, Distorting, and Apparent Components

Based on this theory, the decomposition of voltages and currents waveforms is made using the Fourier transform, according to the model of Constantin Budeanu [1], who deals only with single-phase quantities.

Other Romanian scientific publications issued mainly in the eight decades of the last century [14,15] provided a generalization of this model to three-phase cases. Due to the cumbersome formulas, it was difficult to implement this decomposition model without modern computers. It is worth mentioning that if the basic functions (voltages, currents) have linear forms, the (re)active and distorting powers are built as bilinear forms making use of tensorial calculus. This is correct from both mathematic and technical points of view. Below, one presents such relations for powers calculations in three-phase systems, along with author comments. This theory is named the Antoniu–Gafencu theory.

2.1.1. Relations Used for the Definitions of Active, Reactive and Distorting Powers in a Balanced Three-Phase System Operating in a Distorting Regime

As mentioned above, the tensorial calculus can be used to determine the definition relations for (re)active and distorting power at three-phase systems which operate in (non)symmetric distorting regimes. One has to consider the instantaneous values of the periodic, non-sinusoidal three-phase voltages $u_1(t)$, $u_2(t)$, and $u_3(t)$ that are applied to a balanced receiver that absorbs the currents $i_1(t)$, $i_2(t)$, $i_3(t)$.

One denotes by U_k—the RMS value of the k-th harmonic component of voltage and by γ_k its initial phase-shift. Then the direct symmetrical three-phase system of non-sinusoidal voltages, expressed with the Fourier series, is [14]:

$$\begin{cases} u_1(t) = \sum_0^n \left(\sqrt{2}\cdot U_k\cdot cos\gamma_k\cdot \sin k\omega t + \sqrt{2}\cdot U_k \sin\gamma_k\cdot cosk\omega t\right) \\ u_2(t) = \sum_0^n \left(\sqrt{2}\cdot U_k\cdot cos\left(\gamma_k - k\cdot\frac{2\pi}{3}\right)\cdot \sin k\omega t + \sqrt{2}\cdot U_k \sin\left(\gamma_k - k\cdot\frac{2\pi}{3}\right)\cdot cosk\omega t\right) \\ u_3(t) = \sum_0^n \left(\sqrt{2}\cdot U_k\cdot cos\left(\gamma_k + k\cdot\frac{2\pi}{3}\right)\cdot \sin k\omega t + \sqrt{2}\cdot U_k \sin\left(\gamma_k + k\cdot\frac{2\pi}{3}\right)\cdot cosk\omega t\right) \end{cases} \quad (1)$$

The currents are also part of a direct symmetrical three-phase system [14]. Using the notations I_k and θ_k for the RMS value of the k-th harmonic component of currents and its initial phase-shift, one gets:

$$\begin{cases} i_1(t) = \sum_0^n \left(\sqrt{2}\cdot I_k\cdot cos\theta_k\cdot \sin k\omega t + \sqrt{2}\cdot I_k \sin\theta_k\cdot cosk\omega t\right) \\ i_2(t) = \sum_0^n \left(\sqrt{2}\cdot I_k\cdot cos\left(\theta_k - k\cdot\frac{2\pi}{3}\right)\cdot \sin k\omega t + \sqrt{2}\cdot I_k \sin\left(\theta_k - k\cdot\frac{2\pi}{3}\right)\cdot cosk\omega t\right) \\ i_3(t) = \sum_0^n \left(\sqrt{2}\cdot I_k\cdot cos\left(\theta_k + k\cdot\frac{2\pi}{3}\right)\cdot \sin k\omega t + \sqrt{2}\cdot I_k \sin\left(\theta_k + k\cdot\frac{2\pi}{3}\right)\cdot cosk\omega t\right) \end{cases} \quad (2)$$

The three-phase systems of voltages and currents defined with the relations (1) and (2) allow for a vectorial representation in the linear vectorial space of trigonometric polynomials [14]. Therefore, one can write:

- for voltages:

$$\begin{cases} U_1 = \sum_0^n \left[K_x\cdot U_k\cdot cos\gamma_k + K_y\cdot U_k\cdot \sin\gamma_k\right] \\ U_2 = \sum_0^n \left[K_x\cdot U_k\cdot cos\left(\gamma_k - k\cdot\frac{2\pi}{3}\right) + K_y\cdot U_k\cdot \sin\left(\gamma_k - k\cdot\frac{2\pi}{3}\right)\right] \\ U_3 = \sum_0^n \left[K_x\cdot U_k\cdot cos\left(\gamma_k + k\cdot\frac{2\pi}{3}\right) + K_y\cdot U_k\cdot \sin\left(\gamma_k + k\cdot\frac{2\pi}{3}\right)\right] \end{cases} \quad (3)$$

- for currents:

$$\begin{cases} I_1 = \sum_0^n \left[K_x\cdot I_k\cdot cos\theta_k + K_y\cdot I_k\cdot \sin\theta_k\right] \\ I_2(t) = \sum_0^n \left[K_x\cdot I_k\cdot cos\left(\theta_k - k\cdot\frac{2\pi}{3}\right) + K_y\cdot I_k\cdot \sin\left(\theta_k - k\cdot\frac{2\pi}{3}\right)\right] \\ I_3(t) = \sum_0^n \left[K_x\cdot I_k\cdot cos\left(\theta_k + k\cdot\frac{2\pi}{3}\right) + K_y\cdot I_k\cdot \sin\left(\theta_k + k\cdot\frac{2\pi}{3}\right)\right] \end{cases} \quad (4)$$

where: U_j and Ij (j = l, 2, 3)—represent the vectors (first order tensors) of the phase voltage and current in the vectorial space E,

$$K_x\cdot U_k\cdot cos\gamma_k,\ K_x\cdot U_k\cdot cos\left(\gamma_k - k\cdot\frac{2\pi}{3}\right),\ K_x\cdot U_k\cdot cos\left(\gamma_k + k\cdot\frac{2\pi}{3}\right) \quad (5)$$

represent the projections of the vectors Uj along the axis K_x of a subspace E1 of odd functions (similar equations can be written for currents [14]);

$$K_y\cdot U_k\cdot cos\gamma_k,\ K_y\cdot U_k\cdot cos\left(\gamma_k - k\cdot\frac{2\pi}{3}\right),\ K_y\cdot U_k\cdot cos\left(\gamma_k + k\cdot\frac{2\pi}{3}\right) \quad (6)$$

represent the projections of the vectors Uj along the axis K_y of a subspace E2 of odd functions (similar equations can be written for currents [14]).

In the light of the above, one can determine the expressions for powers in a (non)symmetrical three-phase network that operates in a distorting regime by using the analogy with the definition of these powers in a distorting regime for single-phase cases [1,14,15].

2.1.1.1. Active Powers of Phases and Total Active Power for Phases without Magnetic Couplings

After performing the scalar products between the voltage and current vectors of each phase and considering the orthogonality property of tensors, one gets [14]:

$$\begin{cases} U_1 \cdot I_1 = \sum_0^n U_k \cdot I_k \cdot cos(\gamma_k - \theta_k) = \sum_0^n U_k \cdot I_k \cdot cos\varphi_k \\ U_2 \cdot I_2 = \sum_0^n U_k \cdot I_k \cdot \begin{bmatrix} cos\left(\gamma_k - k \cdot \frac{2\pi}{3}\right) \cdot cos\left(\theta_k - k \cdot \frac{2\pi}{3}\right) + \\ +sin\left(\gamma_k - k \cdot \frac{2\pi}{3}\right) \cdot sin\left(\theta_k - k \cdot \frac{2\pi}{3}\right) \end{bmatrix} = \sum_0^n U_k \cdot I_k \cdot cos\varphi_k \\ U_3 \cdot I_3 = \sum_0^n U_k \cdot I_k \cdot \begin{bmatrix} cos\left(\gamma_k + k \cdot \frac{2\pi}{3}\right) \cdot cos\left(\theta_k + k \cdot \frac{2\pi}{3}\right) + \\ +sin\left(\gamma_k + k \cdot \frac{2\pi}{3}\right) \cdot sin\left(\theta_k + k \cdot \frac{2\pi}{3}\right) \end{bmatrix} = \sum_0^n U_k \cdot I_k \cdot cos\varphi_k \end{cases} \tag{7}$$

where

$$\varphi_k = \gamma_k - \theta_k \tag{8}$$

represents the phase-shift between the voltage and current corresponding to the same harmonic order.

In this way, one gets the expressions for the three equal phase active powers (there is a balanced distribution).

The total active power of the (un)balanced three-phase network operating in a distorting regime can be computed as the sum of the phase active powers [14]:

$$P = U_1 \cdot I_1 + U_2 \cdot I_2 + U_3 \cdot I_3 = P_1 + P_2 + P_3 \tag{9}$$

In the particular case of a balanced receiver, one gets [14]:

$$P = 3 \cdot U_1 \cdot I_1 = 3 \sum\nolimits_0^n U_k \cdot I_k \cdot cos\varphi_k \tag{10}$$

where k represents the harmonic order (associated with the frequency $50 \times k$ in the European system).

2.1.1.2. Reactive Powers of Phases and Total Reactive Power

The expressions for the reactive power of each phase can be obtained by computing the scalar products between the voltages and currents that were previously shifted by $\pi/2$ (in other words, after multiplication with β) [14]:

$$\begin{cases} U_1 \cdot \beta I_1 & = \left[\sum_0^n U_k \cdot \left(K_x \cdot \cos\gamma_k + K_y \cdot \sin\gamma_k\right)\right]\left[\sum_0^n I_k \cdot \left(-K_x \cdot \sin\theta_k + K_y \cdot \cos\theta_k\right)\right] \\ & = \sum_0^n U_k \cdot I_k \cdot sin\varphi_k \\ U_2 \cdot \beta I_2 & = \left\{\sum_0^n U_k \cdot \begin{bmatrix} K_x \cdot \cos\left(\gamma_k - k \cdot \frac{2\pi}{3}\right) + \\ +K_y \cdot \sin\left(\gamma_k - k \cdot \frac{2\pi}{3}\right) \end{bmatrix}\right\}\left\{\sum_0^n I_k \cdot \begin{bmatrix} -K_x \cdot \sin\left(\theta_k - k \cdot \frac{2\pi}{3}\right) + \\ +K_y \cdot \cos\left(\theta_k - k \cdot \frac{2\pi}{3}\right) \end{bmatrix}\right\} \\ & = \sum_0^n U_k \cdot I_k \cdot sin\varphi_k \\ U_3 \cdot \beta I_3 & = \left\{\sum_0^n U_k \cdot \begin{bmatrix} K_x \cdot \cos\left(\gamma_k + k \cdot \frac{2\pi}{3}\right) + \\ +K_y \cdot \sin\left(\gamma_k + k \cdot \frac{2\pi}{3}\right) \end{bmatrix}\right\}\left\{\sum_0^n I_k \cdot \begin{bmatrix} -K_x \cdot \sin\left(\theta_k + k \cdot \frac{2\pi}{3}\right) + \\ +K_y \cdot \cos\left(\theta_k + k \cdot \frac{2\pi}{3}\right) \end{bmatrix}\right\} \\ & = \sum_0^n U_k \cdot I_k \cdot sin\varphi_k \end{cases} \tag{11}$$

The principle of algebraical preservation of reactive powers allows for the following conclusion: the total reactive power of a three-phase system equals the sum of the phase reactive powers [14]:

$$Q = U_1 \cdot \beta I_1 + U_2 \cdot \beta I_2 + U_3 \cdot \beta I_3 \tag{12}$$

This relation is valid for both symmetrical and non-symmetrical systems.

2.1.1.3. Distorting Powers and Their Vectorial Features of Distorting Powers. Total Distorting Power of a Balanced Three-Phase Network in Distorting Regimes

It is known that, in single-phase cases, the distorting power for a dipole represents the absolute value of the vector [14]:

$$\boldsymbol{D} = \frac{1}{\sqrt{2}}(U\Lambda I - \beta U\Lambda\beta I) = \frac{1}{\sqrt{2}}\sum_{k,\ l}\sum\left[d'_{kl}\left(K_x\Lambda l_x - K_y\Lambda l_y\right) + d''_{kl}\left(K_y\Lambda l_x - K_x\Lambda l_y\right)\right] \tag{13}$$

This relation reveals the vectorial feature of the distorting power whilst the absolute value of the vector $\boldsymbol{D}$ represents the known expression of a single-phase receiver's distorting power:

$$D = |\boldsymbol{D}| = \left[\sum_{k,}\sum_{l}\left(d'^2_{kl} + d''^2_{kl}\right)\right]^{\frac{1}{2}} \tag{14}$$

In these relations, d'_{kl} and d''_{kl} represent the elementary distorting powers of the harmonic orders k and l. Under these circumstances, the vectors of the distorting powers for all phases of a three-phase system will be defined based on the linear combinations of the following external products [14]:

$$\begin{aligned}
&\boldsymbol{D}_1 = \tfrac{1}{\sqrt{2}}(U_1\Lambda I_1 - \beta U_1\Lambda\beta I_1) \\
&= \sum_{k,}\sum_{l}\left\{\begin{array}{l} \tfrac{1}{\sqrt{2}}\left[(K_x\Lambda l_x) - \left(K_y\Lambda l_y\right)\right]\cdot\left[U_k\cdot I_l\cdot\cos(\gamma_k+\theta_l) - U_l\cdot I_k\cdot\cos(\gamma_l+\theta_k)\right]+ \\ +\tfrac{1}{\sqrt{2}}\left[\left(K_x\Lambda l_y\right) + \left(K_y\Lambda l_x\right)\right]\cdot\left[U_k\cdot I_l\cdot\sin(\gamma_k+\theta_l) - U_l\cdot I_k\cdot\sin(\gamma_l+\theta_k)\right]\end{array}\right\} \\
&\boldsymbol{D}_2 = \tfrac{1}{\sqrt{2}}(U_2\Lambda I_2 - \beta U_2\Lambda\beta I_2) \\
&= \sum_{k,}\sum_{l}\left\{\begin{array}{l} \tfrac{1}{\sqrt{2}}\left[(K_x\Lambda l_x) - \left(K_y\Lambda l_y\right)\right]\cdot\left[\begin{array}{l} U_k\cdot I_l\cdot\cos\left(\gamma_k+\theta_l - k\cdot\frac{2\pi}{3} - l\cdot\frac{2\pi}{3}\right)- \\ -U_l\cdot I_k\cdot\cos(\gamma_l+\theta_k) - l\cdot\frac{2\pi}{3} - k\cdot\frac{2\pi}{3}\end{array}\right]+ \\ +\tfrac{1}{\sqrt{2}}\left[\left(K_x\Lambda l_y\right) + \left(K_y\Lambda l_x\right)\right]\cdot\left[\begin{array}{l} U_k\cdot I_l\cdot\sin\left(\gamma_k+\theta_l - k\cdot\frac{2\pi}{3} - l\cdot\frac{2\pi}{3}\right)- \\ -U_l\cdot I_k\cdot\sin\left(\gamma_l+\theta_k - l\cdot\frac{2\pi}{3} - k\cdot\frac{2\pi}{3}\right)\end{array}\right]\end{array}\right\} \\
&\boldsymbol{D}_3 = \tfrac{1}{\sqrt{2}}(U_3\Lambda I_3 - \beta U_3\Lambda\beta I_3) \\
&= \sum_{k,}\sum_{l}\left\{\begin{array}{l} \tfrac{1}{\sqrt{2}}\left[(K_x\Lambda l_x) - \left(K_y\Lambda l_y\right)\right]\cdot\left[\begin{array}{l} U_k\cdot I_l\cdot\cos\left(\gamma_k+\theta_l + k\cdot\frac{2\pi}{3} + l\cdot\frac{2\pi}{3}\right)- \\ -U_l\cdot I_k\cdot\cos(\gamma_l+\theta_k) + l\cdot\frac{2\pi}{3} + k\cdot\frac{2\pi}{3}\end{array}\right]+ \\ +\tfrac{1}{\sqrt{2}}\left[\left(K_x\Lambda l_y\right) + \left(K_y\Lambda l_x\right)\right]\cdot\left[\begin{array}{l} U_k\cdot I_l\cdot\sin\left(\gamma_k+\theta_l + k\cdot\frac{2\pi}{3} + l\cdot\frac{2\pi}{3}\right)- \\ -U_l\cdot I_k\cdot\sin\left(\gamma_l+\theta_k + l\cdot\frac{2\pi}{3} + k\cdot\frac{2\pi}{3}\right)\end{array}\right]\end{array}\right\}
\end{aligned} \tag{15}$$

Equation (15) proves the vectorial features of the phase distorting powers, being represented in the space $\Lambda^2 E$ using well-determined vectors.

In the relations (15), the vectors of the elementary distorting powers d'_{kl} of all phases ($d'k_{l1}$, $d'k_{l2}$ and $d'k_{l3}$) are collinear and their absolute values are equal to the elementary distorting powers of the phases [14]:

$$\begin{aligned}
d'_{kl1} &= U_k{\cdot}I_l{\cdot}cos(\gamma_k+\theta_l) - U_l{\cdot}I_k{\cdot}cos(\gamma_l+\theta_k), \\
d'_{kl2} &= U_k{\cdot}I_l{\cdot}cos\left(\gamma_k+\theta_l - k{\cdot}\tfrac{2\pi}{3} - l{\cdot}\tfrac{2\pi}{3}\right) - U_l{\cdot}I_k{\cdot}cos\left(\gamma_l+\theta_k - k{\cdot}\tfrac{2\pi}{3} - l{\cdot}\tfrac{2\pi}{3}\right), \\
d'_{kl3} &= U_k{\cdot}I_l{\cdot}cos\left(\gamma_k+\theta_l + k{\cdot}\tfrac{2\pi}{3} + l{\cdot}\tfrac{2\pi}{3}\right) - U_l{\cdot}I_k{\cdot}cos\left(\gamma_l+\theta_k + k{\cdot}\tfrac{2\pi}{3} + l{\cdot}\tfrac{2\pi}{3}\right)
\end{aligned} \tag{16}$$

In an analogous way, the vectors of distorting powers d''_{kl} of all phases (d''_{kl1}, d''_{kl2}, and d''_{kl3}) are collinear and their absolute values are equal to the elementary distorting powers of the phases [14]:

$$\begin{aligned}
d''_{kl1} &= U_k{\cdot}I_l{\cdot}cos(\gamma_k+\theta_l) - U_l{\cdot}I_k{\cdot}cos(\gamma_l+\theta_k) \\
d''_{kl2} &= U_k{\cdot}I_l{\cdot}cos\left(\gamma_k+\theta_l - k{\cdot}\tfrac{2\pi}{3} - l{\cdot}\tfrac{2\pi}{3}\right) - U_l{\cdot}I_k{\cdot}cos\left(\gamma_l+\theta_k - k{\cdot}\tfrac{2\pi}{3} - l{\cdot}\tfrac{2\pi}{3}\right) \\
d''_{kl3} &= U_k{\cdot}I_l{\cdot}cos\left(\gamma_k+\theta_l + k{\cdot}\tfrac{2\pi}{3} + l{\cdot}\tfrac{2\pi}{3}\right) - U_l{\cdot}I_k{\cdot}cos\left(\gamma_l+\theta_k + k{\cdot}\tfrac{2\pi}{3} + l{\cdot}\tfrac{2\pi}{3}\right)
\end{aligned} \tag{17}$$

and are orthogonal across the vectors $d'k_{11}$, $d'k_{12}$ and $d'k_{13}$. This reveals once more the algebraic conservation of the elementary distorting powers of the same type for all 3 phases, similar to the vector preservation of the distorting power [14].

The tree-phase elementary distorting powers are equal to the sum of the elementary phase distorting powers because d'_{kl} and d''_{kl} are algebraically preserved and the vectors corresponding to each of the two components are collinear. It means that for the pair of harmonics k and l ($k \neq l$, k, l = 1, 2, . . .), one gets the expressions [14]:

$$\begin{cases} d'_{kl} = d'_{kl1} + d'_{kl2} + d'_{kl3} = \begin{bmatrix} U_k \cdot I_l \cdot cos(\gamma_k + \theta_l) - \\ -U_l \cdot I_k \cdot cos(\gamma_l + \theta_k) \end{bmatrix} \cdot \left[l + 2 \cdot cos(k+l) \cdot \frac{2\pi}{3} \right] \\ d''_{kl} = d''_{kl1} + d''_{kl2} + d''_{kl3} = \begin{bmatrix} U_k \cdot I_l \cdot sin(\gamma_k + \theta_l) - \\ -U_l \cdot I_k \cdot sin(\gamma_l + \theta_k) \end{bmatrix} \cdot \left[l + 2 \cdot cos(k+l) \cdot \frac{2\pi}{3} \right] \end{cases} \tag{18}$$

The algebraic conservation of the elementary powers d'_{kl} and d''_{kl} results in the vectorial conservation for all vectors representing the elementary distorting powers; these vectors belong to the orthogonal plan and have a single common point, O, in the space $\Lambda^2 E$, which is the origin of the vector D [14]:

$$D = \frac{1}{\sqrt{2}} [U_1 \Lambda I_1 - \beta U_1 \Lambda \beta I_1 + U_2 \Lambda I_2 - \beta U_2 \Lambda \beta I_2 + U_3 \Lambda I_3 - \beta U_3 \Lambda \beta I_3] \tag{19}$$

Its absolute value can be computed with:

$$\begin{aligned} D = |\boldsymbol{D}| &= \left[\sum_{k,} \sum_{l} \left(d'^2_{kl} + d''^2_{kl} \right) \right]^{\frac{1}{2}} \\ &= \left\{ \sum_{k,} \sum_{l} \begin{bmatrix} U_k^2 \cdot I_l^2 + U_l^2 \cdot I_k^2 - \\ -2U_k \cdot U_l \cdot I_k \cdot I_l \cdot cos(\varphi_k - \varphi_l) \end{bmatrix} \cdot \left[l + 2 \cdot cos(k+l) \cdot \frac{2\pi}{3} \right]^2 \right\}^{1/2} \end{aligned} \tag{20}$$

Equation (20) represents the general form of the total distorting power of a three-phase system operating in a distorting regime and is not influenced by the neutral point origin.

Considering that in a symmetrical three-phase system operating in a distorting regime, the phase voltages or currents will form symmetrical systems with different successions with respect to the harmonic order, based on (20), one can conclude that:

(a) for (k + l) = 3*m (m = 1, 2, 3, . . .), the distorting power of a symmetrical three-phase system is equal to a phase distorting power multiplied by 3 (similar to the (re)active powers);

(b) for (k + 1) = 3*m + 1 or (k + 1)= 3*m + 2 (m = 0, 1, . . .) the distorting power of the three-phase system is null, even though each phase is associated to a distorting power (identical for all phases at symmetrical systems), which can be computed with [14]:

$$D_1 = D_2 = D_3 = \left\{ \sum_{k,} \sum_{l} \left[U_k^2 \cdot I_l^2 + U_l^2 \cdot I_k^2 - 2U_k \cdot U_l \cdot I_k \cdot I_l \cdot cos(\varphi_k - \varphi_l) \right] \right\}^{1/2} \tag{21}$$

This proves that there is a self-compensation of the distorting powers in the symmetrical three-phase system operating in a distorting regime.

Based on these conclusions, one can state that in a symmetrical three-phase system, the total distorting power is lower than the sum of the phase distorting powers [14]:

$$D < D_1 + D_2 + D_3 \tag{22}$$

Obviously, considering Equations (7), (11), (15) and (20), one can state that the total apparent power of a three-phase system is lower than the sum of phases' apparent powers ($S = (P^2 + Q^2 + D^2)^{1/2}$) [14]. Therefore the following relation can be written [14]:

$$S < S_1 + S_2 + S_3 \tag{23}$$

The total power factor measures the relationship between the active power under ideal operating conditions and S [14]:

$$PF_T = \frac{P}{S} \tag{24}$$

where P represents the active power of all phases.

Comments:

(a) One can define in this theory ("Antoniu–Gafencu" theory) the (re)active, distorting and apparent powers by using the separation of power components according to Budeanu's theory for single-phase systems.

(b) Despite Equation (20), one can evaluate the total distorting power as the sum of phase distorting powers. The experience proved that the results yielded by Equations (19) and (20) are close to the sum $D_1 + D_2 + D_3$. As a consequence, one can determine the total apparent power with $S = \left(P^2 + Q^2 + D^2\right)^{1/2}$ and evaluate the power factor with (24).

(c) The results yielded by Equations (7), (11), (15) and (20) provide modalities for measuring, charging, compensation and correct definition of some PQ indices before and after compensation, from both technical and economic points of view.

(d) Distorting powers diminishing actually assumes the diminishing of harmonic power components from voltages and currents with different harmonic orders. This process is followed by a diminishing of high harmonic components from the spectrum of (re)active powers.

2.1.2. Defining the Active, Reactive and Distorting Powers in a Non-Symmetrical Three-Phase System Considering the Symmetrical Voltage and Current Components

The (re)active and distorting powers for unbalanced receivers that operate in a distorting regime can be defined considering the symmetrical voltage and current components making use of a tensorial method, similar to that used in Section 2.1.1.

For this aim, one should consider a non-symmetrical three-phase system consisting of three non-sinusoidal quantities, represented in the vector space E using the vectors V_1, V_2, V_3. In E, the vectors representing the harmonics of order k form a system of three coplanar vectors, for which the theory of symmetrical components is applicable (these components are represented by vectors in the plan k). This is valid for any harmonic order from the system (k = 0, l, . . .).

Owing to the linearity of the transformation in the space E, the expressions used to determine V_0, V_+ and V_- are:

$$\begin{cases} V_0 = \frac{1}{3}\cdot(V_1 + V_2 + V_3) \\ V_+ = \frac{1}{3}\cdot\left(V_1 + a\cdot V_2 + a^2\cdot V_3\right) \\ V_- = \frac{1}{3}\cdot\left(V_1 + a^2\cdot V_2 + a\cdot V_3\right) \end{cases} \tag{25}$$

where a is the rotation operator $a = e^{j\frac{2\pi}{3}}$ which can be used as a multiplicator to the fundamental versors in a plan as follows:

$$\begin{cases} a\cdot K_x = -\frac{1}{2}K_x + \frac{\sqrt{3}}{2}K_y \\ a\cdot K_y = -\frac{\sqrt{3}}{2}K_x + \frac{1}{2}K_y \\ a^2\cdot K_x = -\frac{1}{2}K_x - \frac{\sqrt{3}}{2}K_y \\ a^2\cdot K_y = \frac{\sqrt{3}}{2}K_x - \frac{1}{2}K_y \end{cases} \tag{26}$$

The operator a can be rewritten with respect to the operator β:

$$\begin{cases} a = -\frac{1}{2} + \frac{\sqrt{3}}{2}\cdot\beta \\ a^2 = -\frac{1}{2} - \frac{\sqrt{3}}{2}\cdot\beta \end{cases} \tag{27}$$

Let us consider a three-phase unbalanced receiver characterized by the phase voltages $u_1(t)$, $u_2(t)$, $u_3(t)$, which absorbs the currents $i_1(t)$, $i_2(t)$, $i_3(t)$ in a distorting regime. The non-sinusoidal quantities, submitted to a Fourier decomposition, are approximated through trigonometric polynomials e, being represented in the E by the vectors U_1, U_2, U_3 and respectively I_1, I_2, I_3. These vectors and their symmetrical components have a common origin, which concurs with the origin of space E. The vectors associated with the current/voltage harmonics of order k, along with the corresponding vectors of the symmetrical components of these harmonics for phases, will be placed in the same plan k.

Similarly, the vectors associated with the current/voltage harmonics of order l, along with the corresponding vectors of the symmetrical components of these harmonics for phases, will be placed in the same plan l. The plans k and l are orthogonal.

The phase indices will be denoted by 1, 2, 3, while +, −, 0 represent the indices of the sequences for the direct, inverse and zero-sequence (homopolar) components. Then one can write:

- for corresponding voltages:

(a) positive sequence:

$$\begin{cases} U_{+1} = U_+ = \sum_0^n \left(K_x \cdot U_{+_k} \cdot cos\gamma_{+_k} + K_y \cdot U_{+_k} \cdot \sin\gamma_{+_k}\right) = \sum_0^n \left(K_x \cdot U'_{+_k} + K_y \cdot U''_{+_k}\right) \\ U_{+2} = a^2 \cdot U_+ = -\frac{1}{2}U_+ - \frac{\sqrt{3}}{2} \cdot \beta \cdot U_+ \\ U_{+3} = a \cdot U_+ = -\frac{1}{2}U_+ + \frac{\sqrt{3}}{2} \cdot \beta \cdot U_+ \end{cases} \tag{28}$$

(b) negative sequence:

$$\begin{cases} U_{-1} = U_- = \sum_0^n \left(K_x \cdot U_{-_k} \cdot cos\gamma_{-_k} + K_y \cdot U_{-_k} \cdot \sin\gamma_{-_k}\right) = \sum_0^n \left(K_x \cdot U'_{-_k} + K_y \cdot U''_{-_k}\right) \\ U_{-2} = a \cdot U_- = -\frac{1}{2}U_- + \frac{\sqrt{3}}{2} \cdot \beta \cdot U_- \\ U_{-3} = a^2 \cdot U_- = -\frac{1}{2}U_- - \frac{\sqrt{3}}{2} \cdot \beta \cdot U_- \end{cases} \tag{29}$$

(c) zero sequence:

$$U_{01} = U_{02} = U_{03} = U_0 = \sum_0^n \left(K_x \cdot U_{0_k} \cdot cos\gamma_{0_k} + K_y \cdot U_{0_k} \cdot sin\gamma_{0_k}\right) = \sum_0^n \left(K_x \cdot U'_{0_k} + K_y \cdot U''_{0_k}\right) \tag{30}$$

- for the corresponding currents:

(a) positive sequence:

$$\begin{cases} I_{+1} = I_+ = \sum_0^n \left(K_x \cdot I_{+_k} \cdot cos\theta_{+_k} + K_y \cdot U_{+_k} \cdot \sin\theta_{+_k}\right) = \sum_0^n \left(K_x \cdot I'_{+_k} + K_y \cdot I''_{+_k}\right) \\ I_{+2} = a^2 \cdot I_+ = -\frac{1}{2}I_+ - \frac{\sqrt{3}}{2} \cdot \beta \cdot I_+ \\ I_{+3} = a \cdot I_+ = -\frac{1}{2}I_+ + \frac{\sqrt{3}}{2} \cdot \beta \cdot I_+ \end{cases} \tag{31}$$

(b) negative sequence:

$$\begin{cases} I_{-1} = I_- = \sum_0^n \left(K_x \cdot I_{-_k} \cdot cos\theta_{-_k} + K_y \cdot I_{-_k} \cdot \sin\theta_{-_k}\right) = \sum_0^n \left(K_x \cdot I'_{-_k} + K_y \cdot I''_{-_k}\right) \\ I_{-2} = a \cdot I_- = -\frac{1}{2}I_- + \frac{\sqrt{3}}{2} \cdot \beta \cdot I_- \\ I_{-3} = a^2 \cdot I_- = -\frac{1}{2}\text{-}\frac{\sqrt{3}}{2} \cdot \beta \cdot I_- \end{cases} \tag{32}$$

(c) zero sequence:

$$\begin{aligned} I_{01} = I_{02} = I_{03} = I_0 \quad &= \sum_0^n \left(K_x \cdot I_{0_k} \cdot cos\theta_{0_k} + K_y \cdot I_{0_k} \cdot sin\theta_{0_k}\right) \\ &= \sum_0^n \left(K_x \cdot I'_{0_k} + K_y \cdot I''_{0_k}\right)'' \end{aligned} \tag{33}$$

2.1.2.1. Expression of Active Power with Respect to the Symmetrical Components of Voltage and Current

The total active power can be computed as a sum between the scalar products of the paired voltage and current phase vectors:

$$P = U_1 \cdot I_1 + U_2 \cdot I_2 + U_3 \cdot I_3 \tag{34}$$

or, taking into account the scalar product rules, one can get the total active power of a three-phase system using the symmetrical components:

$$P = 3 \cdot U_0 \cdot I_0 + 3 \cdot U_+ \cdot I_+ + 3 \cdot U_- \cdot I_- \tag{35}$$

Given the expressions for the voltage/current symmetrical components computed with (28)–(33), one will get the total active power of an unbalanced three-phase system operating in a distorting regime:

$$\begin{aligned} P &= 3 \cdot \sum_0^n \left[U'_{0_k} \cdot I'_{0_k} + U''_{0_k} \cdot I''_{0_k} + U'_{+_k} \cdot I'_{+_k} + U''_{+_k} \cdot I''_{+_k} + U'_{-_k} \cdot I'_{-_k} + U''_{-_k} \cdot I''_{-_k} \right] \\ &= 3 \cdot \sum_0^n \left[U_{0_k} \cdot I_{0_k} \cdot cos\varphi_{0_k} + U_{+_k} \cdot I_{+_k} \cdot cos\varphi_{+_k} + U_{-_k} \cdot I_{-_k} \cdot cos\varphi_{-_k} \right] \end{aligned} \tag{36}$$

Obviously, for a non-symmetrical three-phase system operating in a sinusoidal regime, one gets the well-known expression:

$$P = 3 \cdot U_0 \cdot I_0 \cdot cos\varphi_0 + 3 \cdot U_+ \cdot I_+ cos\varphi_+ + 3 \cdot U_- \cdot I_- cos\varphi_- \tag{37}$$

2.1.2.2. Expression of Reactive Power with Respect to the Symmetrical Components of Voltage and Current

The phase reactive powers can be obtained by using the scalar products between the phase voltages and the phase currents (shifted by $\pi/2$, which is multiplied by β). The first one has to compute:

$$\begin{cases} \beta \cdot I_1 = \beta \cdot I_0 + \beta \cdot I_+ + \beta \cdot I_- \\ \beta \cdot I_2 = \beta \cdot I_0 + \beta \cdot a^2 \cdot I_+ + \beta \cdot a \cdot I_- \\ \beta \cdot I_3 = \beta \cdot I_0 + \beta \cdot a \cdot I_+ + \beta \cdot a^2 \cdot I_- \end{cases} \tag{38}$$

and then the total reactive power of the three-phase system will be obtained with:

$$Q = U_1 \cdot \beta I_1 + U_2 \cdot \beta I_2 + U_3 \cdot \beta I_3 \tag{39}$$

or, taking into account the symmetrical components one gets:

$$Q = 3 \cdot U_0 \cdot \beta I_0 + 3 \cdot U_+ \cdot \beta I_+ + 3 \cdot U_- \cdot \beta I_- \tag{40}$$

or:

$$\begin{aligned} Q &= 3 \sum_0^n \left[U''_{0_k} \cdot I'_{0_k} - U'_{0_k} \cdot I''_{0_k} + U''_{+_k} \cdot I'_{+_k} - U'_{+_k} \cdot I''_{+_k} + U''_{-_k} \cdot I'_{-_k} - U'_{-_k} \cdot I''_{-_k} \right] \\ &= 3 \sum_0^n \left[U_{0_k} \cdot I_{0_k} \cdot sin\varphi_{0_k} + U_{+_k} \cdot I_{+_k} \cdot sin\varphi_{+_k} + U_{-_k} \cdot I_{-_k} \cdot sin\varphi_{-_k} \right] \end{aligned} \tag{41}$$

Obviously, for a non-symmetrical three-phase system operating in a sinusoidal regime, one gets the well-known expression:

$$Q = 3 \cdot U_0 \cdot I_0 \cdot sin\varphi_0 + 3 \cdot U_+ \cdot I_+ \cdot sin\varphi_+ + 3 \cdot U_- \cdot I_- \cdot sin\varphi_- \tag{42}$$

2.1.2.3. Expression of Distorting Power with Respect to the Symmetrical Components of Voltage and Current. Vectorial Feature of the Distorting Power in Non-Symmetrical Three-Phase Networks

If one uses the external product space $\Lambda^2 E$ [14,15], the distorting power can also be expressed by using the voltage/current symmetrical components as explained below:

$$\boldsymbol{D} = \frac{3}{\sqrt{2}}\left[U_0 \Lambda I_0 - \beta U_0 \Lambda \beta I_0 + U_+ \Lambda^{-} \beta U_+ \Lambda \beta I_- + U_- \Lambda I_+ - \beta U_- \Lambda \beta I_+\right] \tag{43}$$

or with the relation

$$\boldsymbol{D} = \frac{3}{\sqrt{2}} \sum\nolimits_{k,} \sum\nolimits_{l} \begin{bmatrix} \left(K_x \Lambda l_x - K_y \Lambda l_y\right) \cdot \left(d'_{00_{kl}} + d'_{+-_{kl}} + d'_{-+_{kl}}\right) + \\ + \left(K_x \Lambda l_y - K_y \Lambda l_x\right) \cdot \left(d''_{00_{kl}} + d''_{+-_{kl}} + d''_{-+_{kl}}\right) \end{bmatrix} \tag{44}$$

The following relations explain the modality to compute some terms in (44):

$$\begin{cases} d'_{00_{kl}} = U'_{0_k} \cdot I'_{0_l} - U'_{0_l} \cdot I'_{0_k} - U''_{0_k} \cdot I''_{0_l} + U''_{0_l} \cdot I''_{0_k} \\ d''_{00_{kl}} = U'_{0_k} \cdot I''_{0_l} - U''_{0_l} \cdot I'_{0_k} + U''_{0_k} \cdot I'_{0_l} + U'_{0_l} \cdot I''_{0_k} \\ d'_{+-_{kl}} = U'_{+_k} \cdot I'_{-_l} - U'_{+_l} \cdot I'_{-_k} - U''_{+_k} \cdot I''_{-_l} + U''_{+_l} \cdot I''_{-_k} \end{cases} \tag{45}$$

Based on the expressions found for the (re)active and distorting powers, one can state that in a non-sinusoidal and non-symmetrical three-phase system, the total distorting power is lower than the sum of the phase distorting powers (or the distorting power of a phase multiplied by (3), due to the cancellation of some of the distorting power components, according to the conclusion of previous subsections.

It means that:

$$D < D_1 + D_2 + D_3 \tag{46}$$

where D is given by Equation (44), and D_1, D_2, D_3 represent the distorting powers of phases.

Equation (44) represents the general expression of the total phase distorting powers distorting power of a three-phase system operating in a distorting and non-symmetrical regime [15].

Considering Equations (36), (41) and (44), one can say that the total apparent power of a three-phase system is lower than the sum of phases' apparent powers ($S = \left(P^2 + Q^2 + D^2\right)^{1/2}$) [15]. Therefore, the following relation can be written [15]:

$$S < S_1 + S_2 + S_3 \tag{47}$$

The total power factor measures the relationship between the active power under ideal operating conditions and S:

$$PF_T = \frac{P}{S} \tag{48}$$

where P represents the active power of all phases.

At this point, one can conclude that the proposed definitions for the total apparent power and global power factor for a three-phase receiver:

(a) make possible both the apparent powers and power factor measurement, allowing for the accomplishment of a full load compensation, which involves the following steps: (a1) removing the high order harmonics from the currents and voltages non-sinusoidal waveforms; (a2) symmetrisation of consumers by using symmetrisation schematics on the fundamental harmonic (e.g., Steinmetz connection); (a3) improving the power factor for the fundamental harmonic.

(b) make possible the issuing of definitions for (b1) certain parameters to be used for the quantification of the full load compensation effect; (b2) indices related to the economic effects and the ROI associated with the equipment used during the compensation process.

2.2. Powers Definition Addressed by the IEEE Standard 1459-2010

IEEE 1459-2010 standard [16] provides definitions for powers in unbalanced and nonlinear regimes. Based on them, improvements were provided in a series of previous works [7,13]. For example, to make these theories coherent, in [11], one modified the definitions of V_e and I_e as explained below.

For I_e one defines the total Root Mean Square (RMS) value, the RMS for the fundamental harmonic and the RMS value harmonics at four-wire systems with the following equations [16]:

$$I_e = \sqrt{(I^2{}_{e1} + I^2{}_{eH})/3} \tag{49}$$

$$I_{e1} = \sqrt{(I^2{}_{a1} + I^2{}_{b1} + I^2{}_{c1} + I^2{}_{n1})/3} \tag{50}$$

$$I_{eH} = \sqrt{(I^2{}_{aH} + I^2{}_{bH} + I^2{}_{cH} + I^2{}_{nH})/3} = \sqrt{I^2{}_e - I^2{}_{e1}} \tag{51}$$

For three-wire systems, $I_{n1} = I_{nH} = 0$ and the expressions become simpler [16]:

$$I_e = \sqrt{(I^2{}_{e1} + I^2{}_{eH})/3} \tag{52}$$

$$I_{e1} = \sqrt{(I^2{}_{a1} + I^2{}_{b1} + I^2{}_{c1})/3} \tag{53}$$

$$I_{eH} = \sqrt{(I^2{}_{aH} + I^2{}_{bH} + I^2{}_{cH})/3} = \sqrt{I^2{}_e - I^2{}_{e1}} \tag{54}$$

The practical expressions for the RMS values at voltages are obtained in a similar manner for fore-wire systems [16]:

$$V_e = \sqrt{(V^2{}_{e1} + V^2{}_{eH})} \tag{55}$$

$$V_e = \sqrt{[3(V^2{}_a + V^2{}_b + V^2{}_c) + (V^2{}_{ab} + V^2{}_{bc} + V^2{}_{ca}]/18} \tag{56}$$

$$V_{e1} = \sqrt{[3(V^2{}_{a1} + V^2{}_{b1} + V^2{}_{c1}) + (V^2{}_{ab1} + V^2{}_{bc1} + V^2{}_{ca1}]/18} \tag{57}$$

$$V_{eH} = \sqrt{[3(V^2{}_{aH} + V^2{}_{bH} + V^2{}_{cH}) + (V^2{}_{abH} + V^2{}_{bcH} + V^2{}_{caH}]/18} = \sqrt{V^2{}_{e1} + V^2{}_{e1}} \tag{58}$$

For three-wire systems, obviously, one gets [16]:

$$V_e = \sqrt{(V^2{}_{ab} + V^2{}_{bc} + V^2{}_{ca})/9} \tag{59}$$

$$V_{e1} = \sqrt{(V^2{}_{ab1} + V^2{}_{bc1} + V^2{}_{ca1})/9} \tag{60}$$

$$V_{eH} = \sqrt{(V^2{}_{abH} + V^2{}_{bcH} + V^2{}_{caH})/9} = \sqrt{V^2{}_e - V^2{}_{e1}} \tag{61}$$

This approach, however, does not separate the positive-sequence powers on the fundamental harmonic [16].

$$V_e = \sqrt{V^2{}_a + V^2{}_b + V^2{}_c}/3 \tag{62}$$

$$I_e = \sqrt{I^2{}_a + I^2{}_b + I^2{}_c}/3 \tag{63}$$

With (62) and (63), a new formula for the effective apparent power (S_e) is defined [12,16] the total apparent power as follows:

$$S_e^2 = \left(V^2{}_a + V^2{}_b + V^2{}_c\right)\left(I^2{}_a + I^2{}_b + I^2{}_c\right) = (3V_{e1}I_{e1})^2 \tag{64}$$

which yields to a new expression of the fundamental effective apparent power [16]:

$$S_{e1}^2 = \left(V^2{}_{a1} + V^2{}_{b1} + V^2{}_{c1}\right)\left(I^2{}_{a1} + I^2{}_{b1} + I^2{}_{c1}\right) \tag{65}$$

S_{e1} can also be expressed using the fundamental symmetrical components:

$$S_{e1}^2 = \left[\left(V^+{}_1\right)^2 + \left(V^-{}_1\right)^2 + \left(V^0{}_1\right)^2\right]\left[\left(I^+{}_1\right)^2 + \left(I^-{}_1\right)^2 + \left(I^0{}_1\right)^2\right] \tag{66}$$

With the proposed expressions of V_e, I_e and S_e, the definitions of the new non-symmetrical ("unbalanced" by standard) power and the new non-fundamental effective apparent power are:

$$S_{U1}^2 = S_{e1}^2 - \left(S^+{}_1\right)^2 \tag{67}$$

We consider that it is more appropriate to define this apparent power as a "power of non-symmetry", which is associated with non-symmetrical waveforms (three-phase voltages and currents), rather than to consider it as a "unbalanced" power (used only to characterize the unbalanced receivers!) Even if it is traditional to use the term "unbalanced power", in our opinion, it is correct to use terms like "non-symmetrical power" (or "un-symmetrical/asymmetrical power").

The IEEE 1459-2010 standard separates the apparent power for superior harmonics of voltages and currents as follows [16]:

$$S_{eN}^2 = S_e^2 - S_{e1}^2 = 9\left[\left(V_{e1}^2 \cdot I_{eH}^2\right) + \left(V_{eH}^2 \cdot I_{e1}^2\right) + \left(V_{eH}^2 \cdot I_{eH}^2\right)\right] \tag{68}$$

where: $V_e^2 = V_{e1}^2 + V_{eH}^2$ and $I_e^2 = I_{e1}^2 + I_{eH}^2$.

In this new formula, new terms are defined:

$$S_{eN}^2 = S_e^2 - S_{e1}^2 = D_{e1}^2 + D_{eV}^2 + S_{eH}^2 \tag{69}$$

where one can notice:

- a term corresponding to fundamental equivalent voltage and superior harmonics of currents:
$$D_{e1} = 3V_{e1} \cdot I_{eH} \tag{70}$$
- a term corresponding to fundamental equivalent current and superior harmonics of voltages:
$$D_{eV} = 3V_{eH} \cdot I_{e1} \tag{71}$$
- a term corresponding to the superior harmonics of equivalent voltages and currents:
$$S_{eH} = 3 \cdot V_{eH} \cdot I_{eH} \tag{72}$$

The IEEE 1459-2010 standard defines an active power associated with the superior harmonic orders for voltage and current (P_{eH}) and a so-called "global power" (D_{eH}) by using the following relations [16]:

$$D_{eH} = \sqrt{{S_{eH}}^2 - P^2{}_{eH}} \tag{73}$$

Global terms can be defined as follows [16]:

- Equivalent harmonic distortion of the three-phase voltages:

$$\mathrm{THD}_{eV} = \frac{V_{eH}}{V_{e1}} \tag{74}$$

- Equivalent harmonic distortion of three-phase currents:

$$\mathrm{THD}_{eI} = \frac{I_{eH}}{I_{e1}} \tag{75}$$

Then, based on the above, practical expressions for the nonfundamental apparent power S_{eN} and its components D_{eI}, De_V, and S_{eH} can be obtained [16]:

$$S_{eN} = \sqrt{\mathrm{THD}_{eI}^2 + \mathrm{THD}_{eV}^2 + (\mathrm{THD}_{eI} \cdot \mathrm{THD}_{eV})^2} \tag{76}$$

where:

$$D_{eI} = S_{e1}(\mathrm{THD}_{eI}) \tag{77}$$

$$D_{eV} = S_{e1}(\mathrm{THD}_{eV}) \tag{78}$$

$$S_{eH} = S_{e1}(\mathrm{THD}_{eV})(\mathrm{THD}_{eI}) \tag{79}$$

For systems with $\mathrm{THD}_{eV} \leq 5\%$ and $\mathrm{THD}_{eI} \geq 40\%$, the following approximation is recommended ([16]):

$$S_{eN} = S_{e1}(\mathrm{THD}_{eI}) \tag{80}$$

The load unbalance can be evaluated using the following fundamental unbalanced power:

$$S_{U1} = \sqrt{{S_{e1}}^2 - {S^+{}_1}^2} \tag{81}$$

where $S^+{}_1$ is the fundamental positive-sequence apparent power (VA).

It is important to mention that, owing to the coupling between sequence components for different sequences (+, − or 0), this power might contain additional components apart from those specific to the ordinary sequences. The phenomenon is similar to what is happening in the three-phase network with the harmonics of different orders from voltages and currents! [17]. *From this point of view, one has to notice that some of the power components from S_{U1} are neglected* [17].

The fundamental positive-sequence apparent power $S^+{}_1$ is computed based on two components [16]:

$$S^+{}_1 = \sqrt{(P^+{}_1)^2 + (Q^+{}_1)^{\,2}} \tag{82}$$

where:

$$P^+{}_1 = 3\ V^+{}_1 \cdot I^+{}_1 \tag{83}$$

$$Q^+{}_1 = 3\ V^+{}_1 \cdot I^+{}_1 \cdot sin\theta^+{}_1 \tag{84}$$

The fundamental positive-sequence power factor is computed with [16]:

$$PF_1^+ = \frac{P_1^+}{S_1^+} \tag{85}$$

and plays the same significant role as that played by the fundamental power factor in non-sinusoidal single-phase systems.

The power factor is [16]:

$$PF_e = \frac{P}{S_e} \tag{86}$$

In this theory, the power factor and total harmonic distortion are "factors of merit" for the electrical systems. IEEE Standard 1459-2010 defines the effective power factor (P_{Fe}), the fundamental positive-sequence power factor (P^{+}_{F1}), and the equivalent total harmonic distortions (THD_{eV} and THD_{eI}) as follows [16]:

$$PF^{+}{}_{1} = \frac{P^{+}{}_{1}}{S^{+}{}_{1}} \tag{87}$$

$$\mathrm{THD}_{eV} = \frac{V_{eH}}{V_{e1}} \tag{88}$$

$$\mathrm{THD}_{eI} = \frac{I_{eH}}{I_{e1}} \tag{89}$$

The total power factor measures the relationship between the active power under ideal operating conditions and Se [16]:

$$PF_{T} = \frac{P^{+}{}_{1}}{S_{e}} \tag{90}$$

The different definitions for the power factor components presented in this subsection do not help with establishing components required by the operations used to compensate for the load that operates in distorting and non-symmetric regimes (Equation (90)). Moreover, they cannot be used to define technical or financial indices with regard to ROIs associated with the dynamic (active) compensation of the three-phase loads that operate in distorting and non-symmetrical regimes.

In their turn, the definitions given for (re)active and apparent powers are worthless when it comes to measuring the powers for a fair charging of the distorting and unbalanced consumers.

2.3. Powers Definition Based on the Decomposition with Wavelet Transforms

In non-sinusoidal situations, power components definitions contained in the IEEE Standard 1459-2000 are based on a frequency-domain approach using Fourier transform (FT). The frequency-domain approach can provide a magnitude-frequency spectrum while losing time-related information. Moreover, the FT carries a heavier computational burden. To overcome these limitations, definitions of power components were reformulated in the wavelet domain using different wavelet decompositions (e.g., DWT, Stationary Wavelet Transform, Wavelet Package Transform (WPT)) [18,19]. When DWT is used, both time and frequency information are preserved whilst the computational time and effort are diminished by dividing the frequency spectrum into bands or levels.

The problem of spectral leakage between wavelet levels can be minimized by suitable choosing the wavelet family along with a suitable mother wavelet. The reformulated definitions could be useful for consumers charging and evaluation of the quality of the supplied electric energy, especially when considering non-steady waveforms where the FT-based power components definitions fail [20].

When the Discrete Wavelet Transform (DWT) is used, firstly, the vector with the components of the analysed waveform (S) is decomposed into vectors associated with components of low frequencies (called "approximations") and, respectively, vectors associated with components of high frequencies (called "details"). Afterwards, successive decompositions of the approximations are made, with no further decomposition of the details. Thus, a Multi-resolution Analysis (MRA) is made (Figure 1—left) [18,20,21].

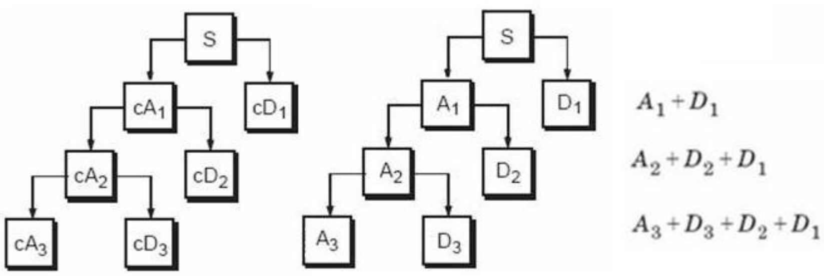

Figure 1. Signal decomposition in approximations and details (**left**) and its re-composition (**right**).

The most significant frequencies from S are characterized by high magnitudes in the vectors of details associated with the level(s) where these frequencies are mapped, with the preservation of their time localization, unlike the case when the Fast Fourier Transform (FFT) is used [22]. The procedure provides a good time resolution at high frequencies and a good frequency resolution at low frequencies [21].

The decomposed signal can be reconstructed with a certain accuracy based on the approximations and details using a schema as that from Figure 1—right (the sign '+' from the schema is used to denote the re-composition).

2.3.1. Power Components Definitions for Single-Phase Waveforms, Based on DWT

Unlike the Fourier transform, Wavelet Transforms allow for time-frequency analysis. Moreover, the condition of symmetry between the semi-periods belonging to a period, assumed by the Fast Fourier Transform, is not imposed on waveforms decomposed with wavelet transforms.

Morsi and his team defined a series of PQ indices for electric signals (voltages and currents). They made analogies with the definitions relying on the Fourier transform, considering the IEEE 1459-2010 Standard [18].

Moreover, starting from the above-mentioned standard, they also defined through analogy various categories of power for single and three-phase cases when the waveforms are distorted [18,19]. Considering the Wavelet transforms, different power component definitions were reformulated [18,19] and new, wavelet-specific PQ indices were introduced.

2.3.1.1. Power Components Definitions When DWT Is Used, Single Phase

1. Calculation of RMS

The following expressions for currents and voltages' RMS values were proposed, starting from the classic definitions for RMS values [18]:

$$V = \sqrt{\frac{1}{T}\int_0^T v^2(t)dt} = \sqrt{\frac{1}{T}\sum\nolimits_k c'^2_{jO,k} + \frac{1}{T}\sum\nolimits_{j\geq jO}\sum\nolimits_k d'^2_{j,k}} = \sqrt{V^2_{jO} + \sum\nolimits_{j\geq jO} V^2_j} \tag{91}$$

$$I = \sqrt{\frac{1}{T}\int_0^T i^2(t)dt} = \sqrt{\frac{1}{T}\sum\nolimits_k c^2_{jO,k} + \frac{1}{T}\sum\nolimits_{j\geq jO}\sum\nolimits_k d^2_{j,k}} = \sqrt{I^2_{jO} + \sum\nolimits_{j\geq jO} I^2_j} \tag{92}$$

where V_{j0}, I_{j0} denotes the RMS values for the level with the lowest frequency $j0$. They are also called "approximation" voltage/current (V_{app}/I_{app}) or the "node zero" voltage/current. $\{Vj\}$, $\{Ij\}$ represent the sets of RMS values for higher frequency bands and are also called "details" voltage/current (V_{det}/I_{det}). Their sum gives the so-called "non-zero nodes" RMS values. $c\prime_{jO,K}$ and $c_{jO,K}$ are the discrete wavelet coefficients corresponding to voltage, respectively, to current for the level j_0, and sample k, whilst $d\prime_{j.k}$ and $d_{j.k}$ are the discrete wavelet coefficients for the levels $j \neq j_0$, sample k [18]:

$$c\prime_{jO,k} = \left\langle v(t), \varphi_{jO,k} \right\rangle, \quad d\prime_{j,k} = \left\langle v(t), \psi_{j,k} \right\rangle \tag{93}$$

$$c_{jO,k} = \left\langle i(t), \varphi_{jO,k} \right\rangle, \quad d_{j,k} = \left\langle i(t), \psi_{j,k} \right\rangle, \tag{94}$$

In the above equations $\varphi_{jO,k}$ represents the scale, $\psi_{j,k}$ represents the wavelet function and "< >" is used to represent the scalar product.

Based on this decomposition for voltage and currents, the next quantities (indices) are defined [18]:

2. Total harmonic distortion

The voltage/current total harmonic distortions calculated with DWT can be defined as [18]:

$$\mathrm{THD}_V = \frac{V_{det}}{V_{app}} = \frac{\sqrt{\sum_{j \geq j_0} V_j^2}}{V_{j_0}} \tag{95}$$

$$\mathrm{THD}_I = \frac{I_{det}}{I_{app}} = \frac{\sqrt{\sum_{j \geq j_0} I_j^2}}{I_{j_0}} \tag{96}$$

3. Active power

The approximation and details of active powers are defined as [18]:

$$P_{app} = P_{j_0} = \frac{1}{T} \cdot \sum_k c'_{j_0,k} \cdot c_{j_0,k} \tag{97}$$

$$P_{det} = \sum_{j \geq j_0} P_j = \frac{1}{T} \cdot \sum_{j \geq j_0} \sum_k d'_{j,k} \cdot d_{j,k} \tag{98}$$

where the total active power is the sum of the above components [18]:

$$P = P_{app} + P_{det} \tag{99}$$

Based on the definition from IEEE 1459-2010 standard, a non-active power N can be calculated using Wavelet Transform with Equation [18]:

$$N = \sqrt{S^2 + P^2} \tag{100}$$

4. Apparent power

The apparent power associated with approximations, S_{app}, is defined as [18]:

$$S_{app} = V_{app} \cdot I_{app} = V_{j_0} \cdot I_{j_0} \tag{101}$$

The definitions, making an analogy with those from the IEEE 1459-2010 Standard, for the current/voltage distorting powers D_I, D_V are [18]:

$$D_I = V_{app} \cdot I_{det} = V_{j_0} \cdot \left(\sqrt{\sum_{j \geq j_0} I_j^2} \right);\ D_V = V_{det} \cdot I_{app} = \left(\sqrt{\sum_{j \geq j_0} V_j^2} \right) \cdot I_{j_0} \tag{102}$$

$$S_{det} = V_{det} \cdot I_{det} = \left(\sqrt{\sum_{j \geq j_0} V_j^2} \right) \cdot \left(\sqrt{\sum_{j \geq j_0} I_j^2} \right) \tag{103}$$

The distorting power of details, D_{det}, is calculated with [18]:

$$D_{det} = \sqrt{S_{det}^2 + P_{det}^2} \tag{104}$$

With the above, the total apparent power S can be calculated with [18]:

$$S^2 = (VI)^2 = S_{app}^2 + D_I^2 + D_v^2 + S_{det}^2 \tag{105}$$

The "non-approximation" apparent power, S_N, is defined as [18]:

$$S_N^2 = D_I^2 + D_v^2 + S_{det}^2 \tag{106}$$

5. Power Factor

The displacement power factor (dPF) is defined as [18]:

$$dPF = \frac{P_{app}}{S_{app}} \tag{107}$$

The total power factor (PF) is calculated as a ratio:

$$PF = \frac{P}{S} \tag{108}$$

The oscillating power factor is computed with [9]:

$$PF_{osc} = \frac{P}{\sqrt{P^2 + \frac{1}{2}S^2}} = \frac{PF}{\sqrt{\frac{1}{2} + PF^2}} \tag{109}$$

6. Details pollution

The pollution associated with "details" DP can be defined as a ratio [18]:

$$DP = \frac{S_N}{S_{app}} \tag{110}$$

As the Discrete Wavelet Transform is to be used, in all the expressions above one should consider 2^N instead of T, where N represents the number of points used for calculation obtained from the interpolation of the acquired samples.

2.3.1.2. Power Components Definitions When DWT Is Used, Three-Phase Systems

1. Calculation of Root Mean Square (RMS) values

The RMS values associated with "approximations" for three-phase voltages and currents were formulated in [19] as:

$$V, I_{eapp} = \sqrt{\frac{V, I^2{}_{RSapp} + V, I^2{}_{STapp} + V, I^2{}_{TRapp}}{3}} \tag{111}$$

As expected, the RMS values associated with "details" are:

$$V, I_{det} = \sqrt{\frac{V, I^2{}_{RSdet} + V, I^2{}_{STdet} + V, I^2{}_{TRdet}}{3}} \tag{112}$$

Then the total RMS values of voltage and current are [19]:

$$V_e = \sqrt{V_{eapp}^2 + V_{edet}^2},\ I_e = \sqrt{I_{eapp}^2 + I_{edet}^2} \tag{113}$$

The definitions for the equivalent voltage (current) harmonic distortions are [19]:

$$\mathrm{THD}_{eV} = \frac{V_{edet}}{V_{eapp}},\ \mathrm{THD}_{eI} = \frac{I_{edet}}{I_{eapp}} \tag{114}$$

2. Active power

When the representation of the symmetrical components is used, the following quantities are defined [19]:

$$i^+ = \frac{1}{3} \cdot [i_R + i'_S + i''_T];\ u^+ = \frac{1}{3} \cdot [u_R + u'_S + u''_T] \tag{115}$$

where the operator' is used to denote a "left-shifted" quantity whilst the operator " is used to denote a "right-shifted" quantity considering a phase-shift of 120°. Therefore, the "approximation" positive sequence active power P_{app}^+ can be defined as [19]:

$$P_{app}^+ = 3\left(\frac{1}{T}\right) \int_0^T v^+ \cdot i^+ dt \tag{116}$$

The total active power of the three-phase systems is then [19]:

$$P = P^{+}_{app} + \sum_{i=1,3} P_{\det_{phasei}} \tag{117}$$

3. Apparent power

The effective apparent power associated with „approximations" S_{eapp} and the unbalanced power associated with "approximations" S_{Uapp} are [19]:

$$S^{+}{}_{app} = 3V^{+}{}_{app}I^{+}{}_{app},\ S_{eapp} = 3V_{eapp}I_{eapp},\ S_{Uapp} = \sqrt{s^{2}{}_{eapp} - \left(S^{+}{}_{app}\right)^{2}} \tag{118}$$

The definitions used for the current/voltage distorting powers and the "apparent power associated with "details" are [19]:

$$D_{eI} = 3V_{eapp}I_{edet},\ D_{eV} = 3V_{edet}I_{eapp},\ S_{edet} = 3V_{edet}I_{edet} \tag{119}$$

The effective apparent power labelled as "non-approximation", S_{eN} is defined as [19]:

$$S_{eN} = \sqrt{D^{2}{}_{eI} + D^{2}{}_{eV} + S^{2}{}_{edet}} \tag{120}$$

The effective apparent power S_e and the nonactive power N are defined as [19]:

$$S_e = \sqrt{S^2_{eapp} + S^2_{eN}},\ N = \sqrt{S^2_e - P^2} \tag{121}$$

4. Power Factor

The positive sequence power factor $PF^{+}{}_{\mathrm{app}}$ is associated with"approximations" and the total power factor PF can be defined as [19]:

$$PF^{+}{}_{app} = \frac{P^{+}{}_{app}}{S^{+}{}_{app}},\ PF = \frac{P}{S_e} \tag{122}$$

5. Details Pollution

The pollution associated with "details", DP, is defined as [19]:

$$DP = \frac{S_{eN}}{S_{eapp}} \tag{123}$$

6. Load Unbalance

The load unbalance can be used to measure the system unbalance and its expression is [19]:

$$LU = \frac{S_{Uapp}}{S^{+}_{app}} \tag{124}$$

2.4. Theory Relying on the Powers' Definition Using the Real and Imaginary Powers Definition

If $u_a(t)$, $u_b(t)$, $u_c(t)$ are the phase voltages of a three-phase load whose modified α, β, 0 components are $u_\alpha(t)$, $u_\beta(t)$, $u_0(t)$ and these voltages supply the load with the currents $i_a(t)$, $i_b(t)$, $i_c(t)$ whose modified α, β, 0 components are $i_\alpha(t)$, $i_\beta(t)$, $i_0(t)$ then the instantaneous real power is defined as [11]:

$$p(t) = u_a(t)i_a(t) + u_b(t)i_b(t) + u_c(t)i_c(t) = p_a(t) + p_b(t) + p_c(t) \tag{125}$$

This instantaneous power can be rewritten under the form [11,12]:

$$p(t) = u_\alpha(t)i_\alpha(t) + u_\beta(t)i_\beta(t) + u_0(t)i_0(t) = p_\alpha(t) + p_\beta(t) + p_0(t) = p_r(t) + p_0(t) \tag{126}$$

where [11,12]:

$$p_r(t) = p_\alpha(t) + p_\beta(t) \tag{127}$$

is the instantaneous real power without zero components and [11,12]:

$$p_0(t) = u_0(t)i_0(t) \tag{128}$$

is the instantaneous zero power.

An advantage of the decomposition in the modified α, β, 0 components consists in the separation of the instantaneous homopolar component from the expression of the instantaneous real power [11].

Akagi and his research team suggested the definition of a new variable [11], called instantaneous imaginary power $q(t)$ or $p_i(t)$, that is not influenced by the zero-sequence components [11]:

$$q(t) = p_i(t) = u_\beta(t)i_\alpha(t) - u_\alpha(t)i_\beta(t) \tag{129}$$

This new power can also be expressed with respect to the line voltages and phase currents:

$$q(t) = \frac{1}{\sqrt{3}}[u_{ab}(t)i_c(t) + u_{bc}(t)i_a(t) + u_{ca}(t)i_b(t)] \tag{130}$$

Under these circumstances, the expressions for $p_r(t)$ and $q(t)$ can also be written using matrices:

$$\begin{bmatrix} p_r(t) \\ q(t) \end{bmatrix} = \begin{bmatrix} u_\alpha(t) & u_\beta(t) \\ u_\beta(t) & -u_\alpha(t) \end{bmatrix} \cdot \begin{bmatrix} i_\alpha(t) \\ i_\beta(t) \end{bmatrix} \tag{131}$$

Each of the instantaneous powers defined here contains an average term and a fluctuating term [11,12]:

$$p(t) = \overline{p} + \widetilde{p}(t)q(t) = \overline{q} + \widetilde{q}(t) \tag{132}$$

Equation (132) reveals what makes the difference to the classic theory: the reactive power is emphasized as an average value of the instantaneous imaginary power.

Based on these definitions, the active and reactive powers, considered as averaged quantities along a period of the real and imaginary instantaneous powers, will be obtained in the following forms [23,24]:

- For the reactive power:

$$q = 3\left[\sum\nolimits_{k=3m+1} U_k I_k sin\phi_k - \sum\nolimits_{k=m3+2} U_k I_k sin\phi_k\right] \tag{133}$$

- The active power can be computed with the formula from Equation (10).

Starting from this approach, the recently issued speciality literature presents a series of variants that use transformations of coordinates toward coordinates for electric quantities, all starting from the p-q theory [25].

A series of power components are analysed in [25] for three-phase systems with 4 wires (the modified p-q formulation, the formulation using the d-q transformation, the p-q-r formulation, the vector formulation).

*However, all these formulations make use of definitions for powers that should provide compensation solutions for the distorting and non-symmetrical effects and do not provide solutions for their measurement and quantification in quantities that should provide solutions for consumers' charging. This theory does not define a global power (e.g., apparent power) and, therefore, there is no power factor associated with it. The attempt to define an apparent power according to the formula s(t) = p(t) + j*q(t) is somehow "forced", as it does not consider any other power components which might appear in non-sinusoidal regimes.*

The mean value of this power along a period should be computed with:

$$S = \sqrt{P^2 + Q^2} \tag{134}$$

revealing that only the mean values along a period of (re)active powers can contribute to the eventual determination of total apparent power. The theory relying on the definition of instantaneous real and imaginary powers relies on the Fourier decomposition of steady signals. As one can see from Equation (133), in this theory, different signs can appear for the reactive power along different superior harmonics and this does not happen in the other theories approached in this paper.

This property might bring certain advantages—for example might help explain the causes for the apparition of some braking torques al rotating electric motors (some reactive power components might be incriminated).

When one turns from the system with 3 axes of coordinates to the system with 2 axes of coordinates and afterwards turns back to the one with 3 axes, this theory can be applied only as fundament for a load compensation when considering the superior harmonics.

Maybe the correct name of this theory should be: ***"The compensation based on the definition using the real and imaginary powers definition"*** *(not as a theory for powers in a three-phase system).*

The diminishing of current harmonic components by using active or hybrid filtering is reduced by default to the voltage harmonics from a three-phase receiver which operates in a non-sinusoidal regime. Despite the ability to diminish voltage and current harmonics, the full load compensation, which should involve the consumer symmetrisation and the improvement of power factor along the fundamental harmonic, cannot be obtained by using this theory!

3. Results

To have a picture of the usability of the definitions presented, real data processing was performed based on these definitions.

Results of decompositions based on FFT (according to the first theory) were compared to those yielded by DWT. The second theory relying on FFT (addressed by the standard IEEE 1459-2010) allows for the definitions of the powers relying on DWT decomposition and, therefore, an algorithm for their determination using it was implemented.

The FFT decomposition computes and takes into consideration all the harmonic orders up to the limit imposed by the Nyquist criterion (which is 100 and, therefore, the limits of 40-th or 50-th harmonic orders imposed by standards are exceeded), but only the components whose weights exceed a threshold imposed by the user (e.g., 1.2%) are displayed. The authors developed original software tools for analysis which use spline interpolations of the vectors of acquired samples to get more accurate results. Voltages and currents from three-phase systems were acquired with dedicated data acquisition systems (DAS), designed and manufactured for the applications presented in this section, with a sampling rate which allowed the estimation of harmonic orders lower than 192. This value is higher than the frequency mentioned by the CISPR standards as being the left margin for frequency ranges associated with Electromagnetic Compatibility issues.

The DWT decomposition provides more accurate results in the case of non-steady signals. Comparisons between quantities defined under the frame of various theories (power quality indices, powers and power factors) were made. A good convergence of results provided by the compared methods was revealed. It means that the first theory (which involves the decomposition into (re)active, distorting and apparent powers) can be used for a correct measurement of the powers/energies in the case of distorting and non-symmetrical waveforms. This theory also allows for the definition of the power factor in three-phase systems, also making possible the charging of distorting and unbalanced consumers.

Harmonic decompositions considering a maximum harmonic order of 192 were made, yielding currents, voltages and powers spectra. FFT decompositions of the acquired electrical signals were used for power computations based on the theoretical support from [12,23,26]. The fundamental harmonic is considered to be equal to 50 Hz.

3.1. Study of Waveforms Acquired from the Secondary Winding of a Transformer Used to Supply the Excitation of a Power Group

3.1.1. Operational Context

The operational context for the first case study refers to a power group which was submitted to technological modifications. In the old system, the excitation was supplied by a synchronous generator by using a three-phase rectifier with thyristors and now the excitation winding was supplied direct from the main generator terminals (G) by using a transformer T to supply the three-phase rectifier with thyristors R which supplied the main generator excitation (Figure 2).

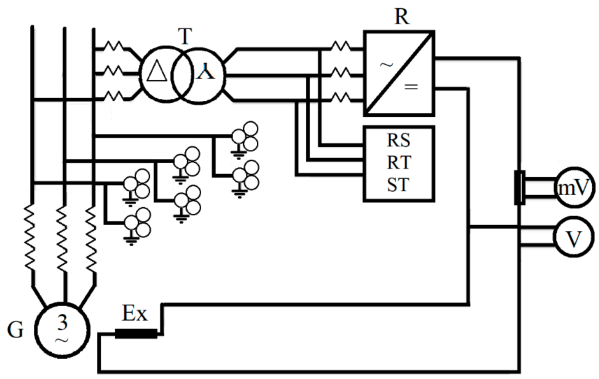

Figure 2. Schematic of a power group with static excitation: G—main generator; T—transformer for the supplying excitation 24/0.65 kV; R—rectifier with controlled thyristors; Ex—excitation winding.

Because there is no galvanic separation, significant non-sinusoidal regimes appeared in the secondary winding of T (SWT) and respectively in the T's primary winding (as transmitted from SWT). Due to these regimes, certain components of the power group were damaged. In this context, the authors designed and realized a complex system for the power group monitoring, which allowed the acquiring of data which were afterwards processed with FFT and DWT. The DASs were adapted such as to be able to acquire electric signals from power systems.

Figure 3 depicts a sequence of 0.03 s. from a set of acquired and processed data (top—voltages, down—currents).

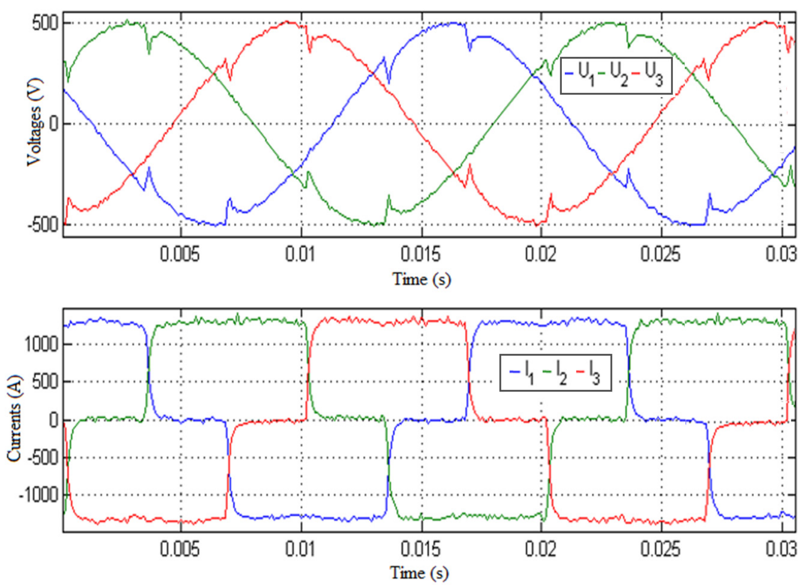

Figure 3. The three-phase voltages and currents acquired in the secondary winding of the transformer for excitation supply.

3.1.2. Data Processing and Powers Computation by Using Fast Fourier Transform

Figure 4 depicts the current and voltage harmonics whose magnitudes exceed 1.2% of the fundamental harmonic's magnitude (one can see that the maximum harmonic order is 43). In all figures representing spectra in this paper, the following convention was used relative to colours: blue—first phase, green—second phase, red—third phase and black—total.

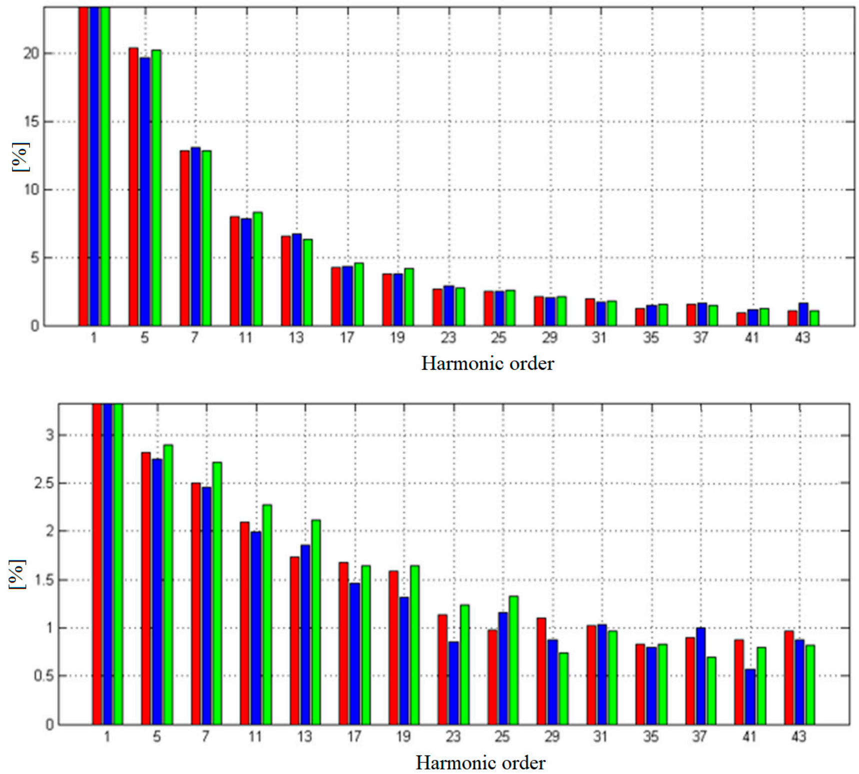

Figure 4. Harmonic spectra of the absorbed currents (**top**) and input voltages (**bottom**) were acquired from the secondary winding of the transformer for the excitation supply (harmonic weights > 1.2%).

The (re)active powers were computed by using the harmonic spectra and Equations (9), (12) and (21). Their spectra are depicted in Figure 5.

Various PQ indices and powers were computed using the mathematical formulations from the previous Section 2.1.1 and the results of numerical harmonic decompositions. The numerical results are gathered in Table 1.

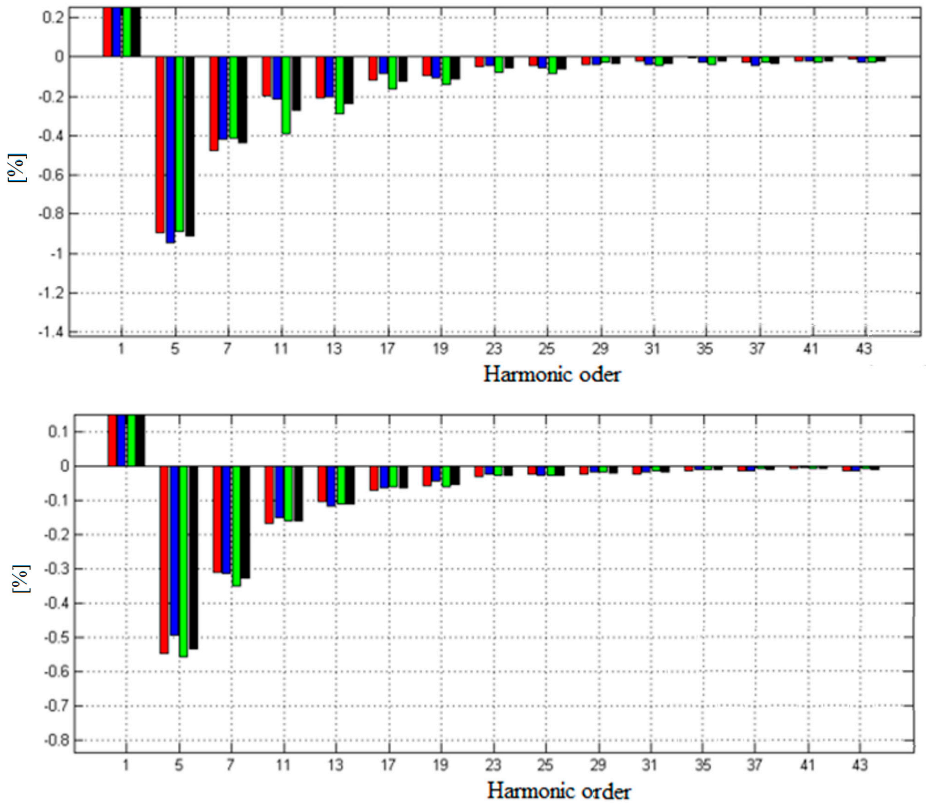

Figure 5. Harmonic spectra of active powers (**top**) and reactive powers (**bottom**) for the secondary winding of the transformer for excitation supply (harmonic weights > 1.2%).

Table 1. Power quality indices, powers and power factors are computed with FFT and the first theory, the first case study.

Index	Units	Phase Number		
		1	2	3
Total RMS of currents	A	1048.85	1053.77	1067.91
RMS of currents for the fundamental harmonic	A	1011.46	1017.03	1029.31
Distorting residue of currents	A	227.47	275.76	283.96
Total harmonic distortion of currents	%	26.46	26.17	26.59
Total RMS of voltages	V	337.55	336.77	333.81
RMS of voltages for the fundamental harmonic	V	336.88	336.18	333.06
Distorting residue of voltages	V	21.27	20.07	22.21
Total harmonic distortion of voltages	%	6.3	5.96	6.65
Phase active powers	kW	96.51	100.28	103.09
Total active power	kW		299.88	
Phase active powers for the fundamental harmonic	kW	98.67	102.62	105.97
Total active power for the fundamental harmonic	kW		307.26	
Phase reactive powers	kVAr	321.59	321.91	321.52
Phase reactive powers on the fundamental harmonic	kVAr	326.14	326.14	326.03
Total reactive power	kVAr		978.36	
Phase distorting powers	kVAd	112.29	110.74	114.32
Total distorting power	kVAd		337.35	
Phase apparent powers	kVA	354.04	354.88	356.76
Phase apparent powers on the fundamental harmonic	kVA	340.74	341.9	342.82
Total apparent power	kVA		1065.4	
Power factor on the fundamental harmonic			0.299 (inductive character)	
Power factor			0.281 (inductive character)	

The analysis of results yielded by the processing of the acquired data characteristic to the rectifier supplying voltages and phase currents obtained from the SWT revealed that:

(a) The voltages harmonic distortions appear because they are used to supply the three-phase rectifier fully controlled by thyristors (TRFCT): ($THDU_1$ = 6.3%; $THDU_2$ = 5.96%; $THDU_3$ = 6.65%).

(b) The phase currents total harmonic distortions are high ($THDI_1$ = 26.46%; $THDI_2$ = 26.17%; $THDI_3$ = 26.59%) because the SWT is used to supply the TRFCT (consisting of 2 rectifier bridges). One can notice significant weights of the current harmonic orders from the set {5, 7, 11, 13, 17, 19, 23} and non-negligible harmonic orders from the set {25, 29, 31, 35, 37, 41, 43}.

A joint analysis of the THDIs and phase currents peak factors revealed significant deviations from the sinusoidal shape.

(c) The total active power from SWT was equal to 299.88 kW whilst the fundamental one was equal to 307.26 kW, revealing a reversed flow of active power along the superior harmonics from the rectifier toward SWT for the excitation supplying.

(d) The total reactive power from SWT was equal to 978.36 kVAr.

(e) The distorting power was significant (equal to 337.35 kVAd) as compared to the active power. The total apparent power was also high (equal to 1065.4 MVA) when compared to the active power whilst its fundamental component was lower than the total apparent power (1025 MVA).

(f) The high values of the apparent, reactive and distorting powers as compared to the active power are reflected by the low value of the total power factor (PF = 0.281).

The analysis of numerical results emphasized the possibility of determining the indices of PQ for powers/energies for three-phase systems by using the first theory discussed above, along with the possibility of determining various categories of powers required for their correct evaluation such as to allow for fair charge and for applying and evaluation of correct compensation measures of non-sinusoidal regimes.

3.1.3. Data Processing and Powers Computation by Using Discrete Wavelet Transform

DWT was used to process the signals depicted in Figure 3. Formulas from Section 2.3.1.2 were used. The topology of the DWT tree used for the results presented in this paper is characterized as follows: 8192 points in the vector hosted by the root node, 10 levels, wavelet mother from the Daubechies family, called 'db4′ in MATLAB, with the filter of length 8. The arguments used to select this topology were: (a) the number of points hosted by the root node is multiple of 2 and it is the closest value to the one used for the computations relying on FFT; (b) the number of points (equal to 8) in the vectors from the 10-th level is equal to the length of the wavelet mother filter; (c) the runtime associated to the DWT decomposition is lower when the filter is shorter; (d) the tests made on synthetic signal revealed an acceptable spectral leakage associated with lower order harmonics, which tend to be partially considered as part of the component oscillating at the fundamental frequency. The percentage relative error between the correct RMS of fundamental and the RMS of fundamental frequency yielded by DWT was highest for the second harmonic order (-0.5%) and decreased significantly with the harmonic order (e.g., -9.6×10^{-3} for the fifth harmonic). For signals with reach harmonic spectra, these sorts of errors tend to compensate each other, whilst for those characterized only by low harmonic orders and small weights, they are more visible with respect to percentage relative error, but the absolute value of errors is small.

The computed vectors of approximations and details for all levels and phases were determined and are depicted in Figures 6–19.

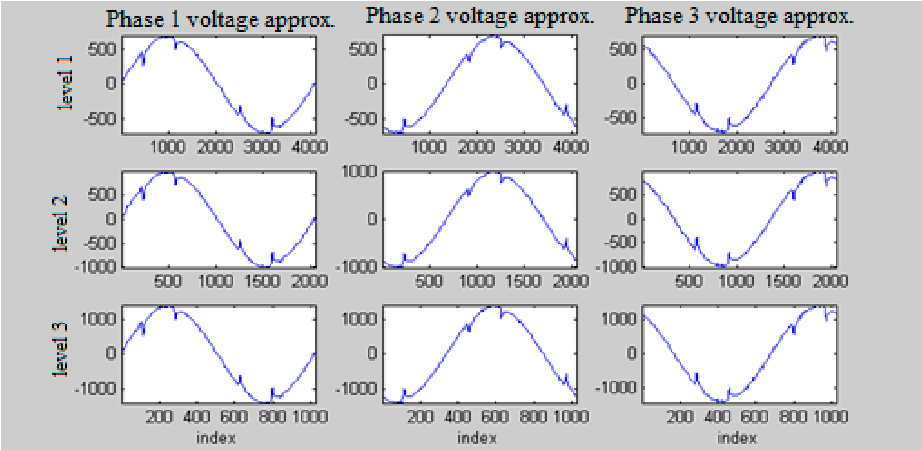

Figure 6. Vectors of approximations for voltages, levels 1–3, first case study.

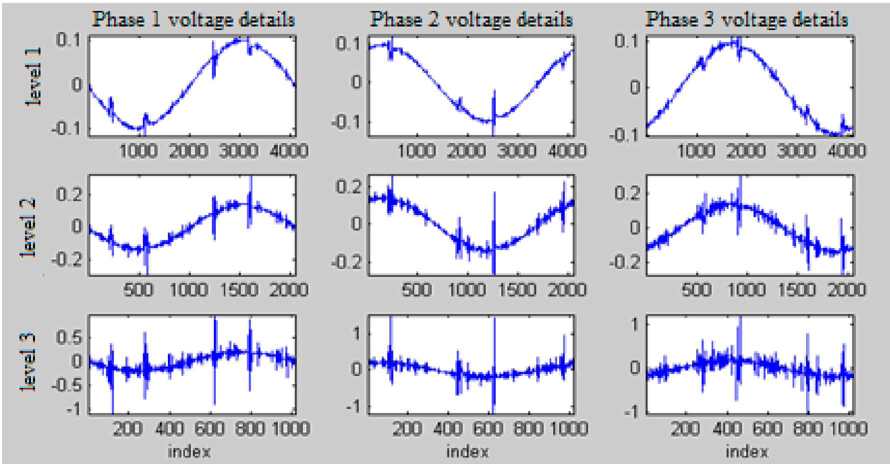

Figure 7. Vectors of details for voltages, levels 1–3, first case study.

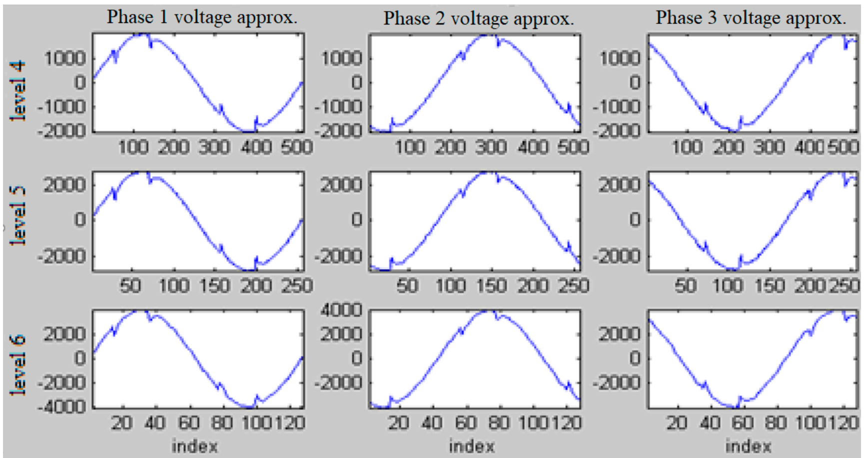

Figure 8. Vectors of approximations for voltages, levels 4–6, first case study

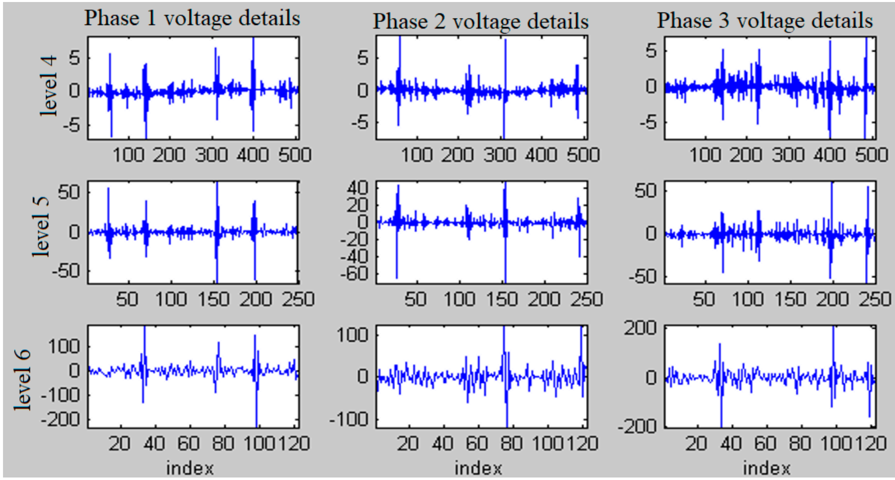

Figure 9. Vectors of details for voltages, levels 4–6, first case study.

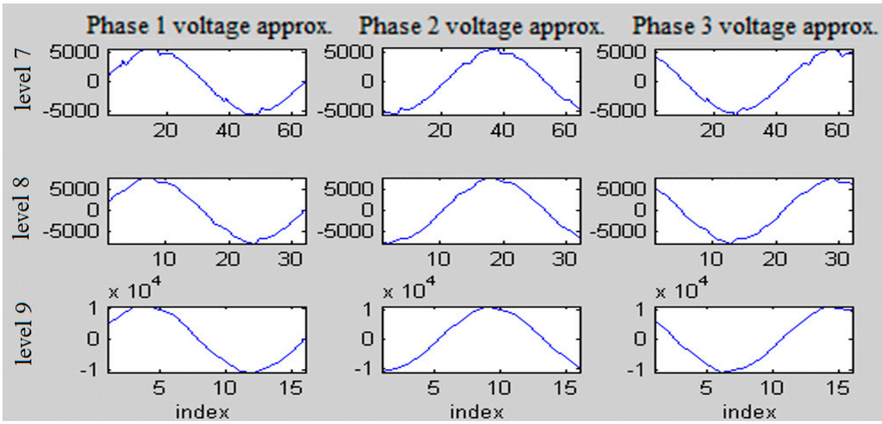

Figure 10. Vectors of approximations for voltages, levels 7–9, first case study.

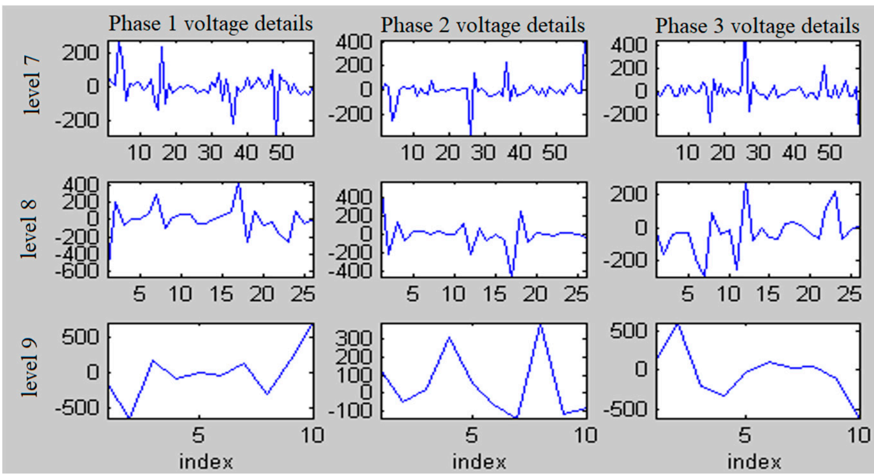

Figure 11. Vectors of details for voltages, levels 7–9, first case study.

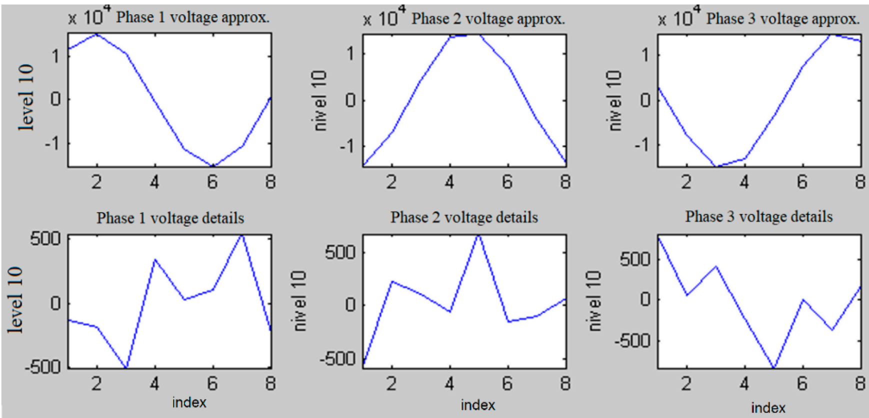

Figure 12. Vectors of approximations and details for voltages, level 10, first case study.

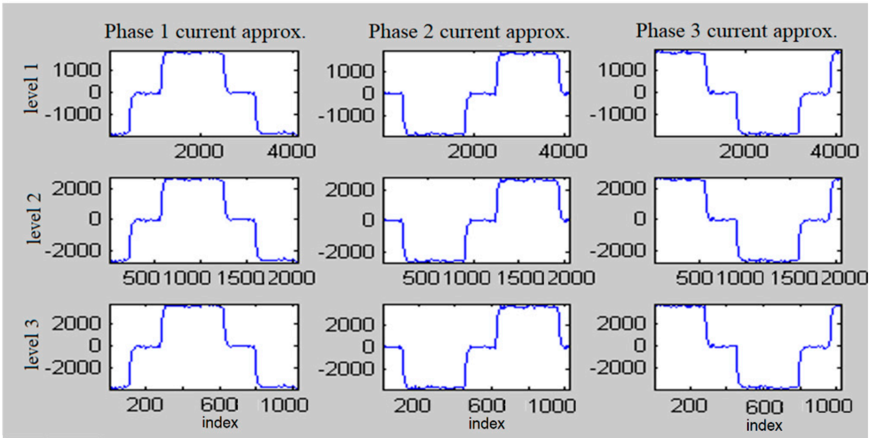

Figure 13. Vectors of approximations for currents, levels 1–3, first case study.

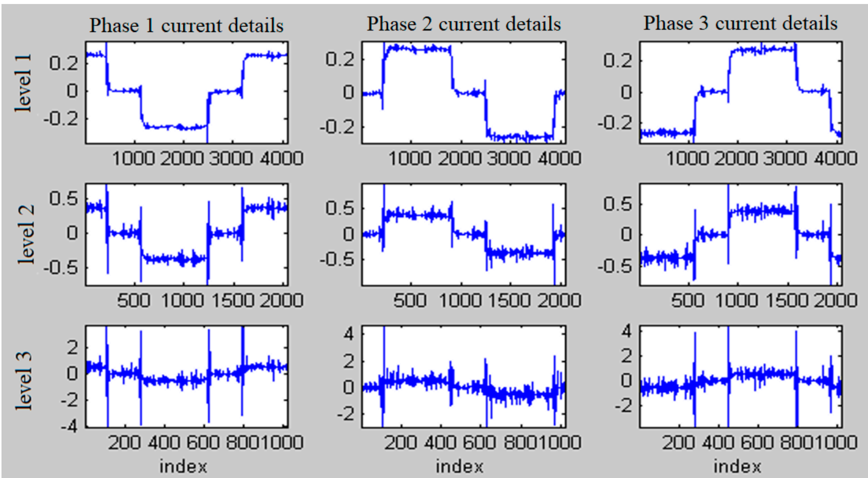

Figure 14. Vectors of details for currents, levels 1–3, first case study.

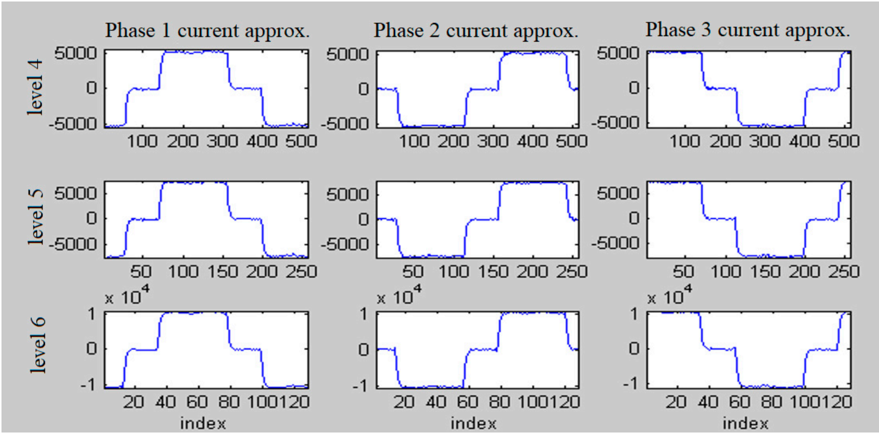

Figure 15. Vectors of approximations for currents, levels 4–6, first case study.

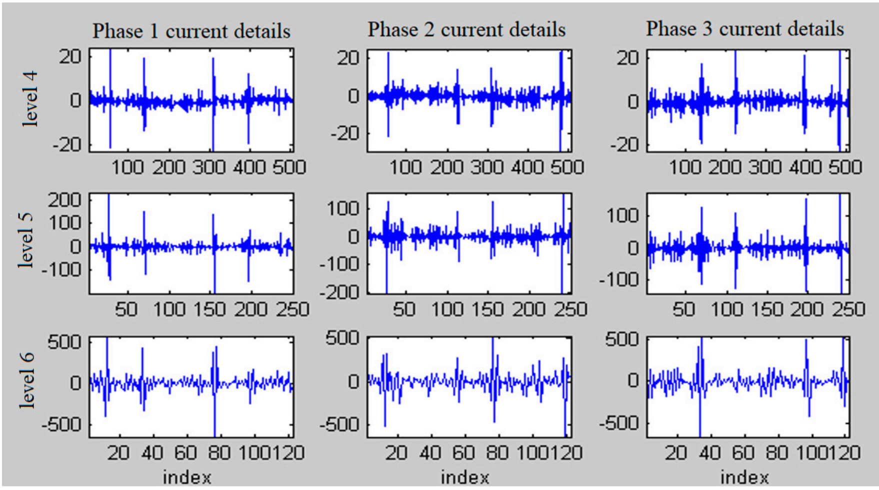

Figure 16. Vectors of details for currents, levels 4–6, first case study.

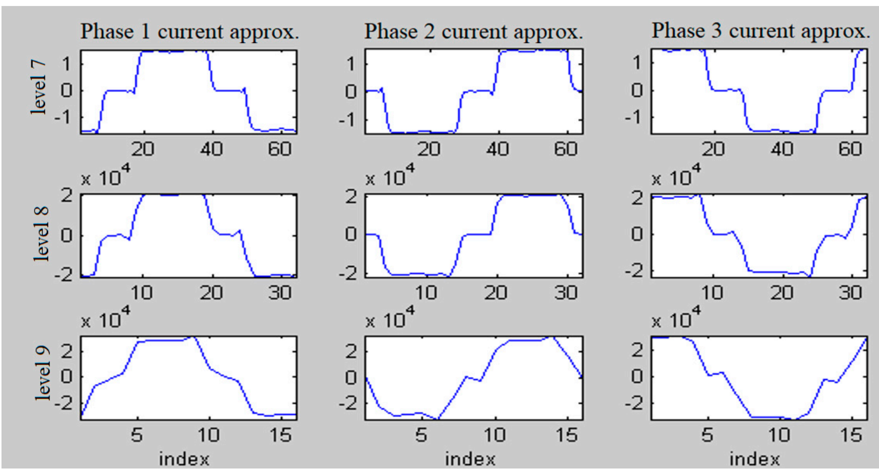

Figure 17. Vectors of approximations for currents, levels 7–9, first case study.

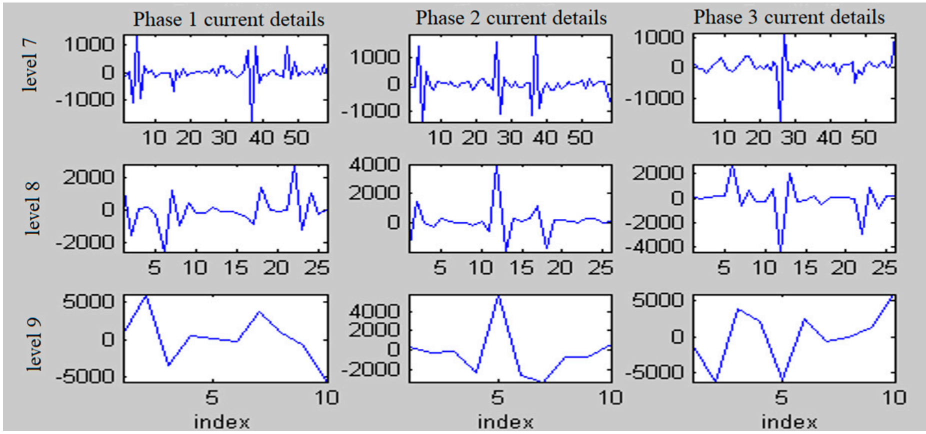

Figure 18. Vectors of details for currents, levels 7–9, first case study.

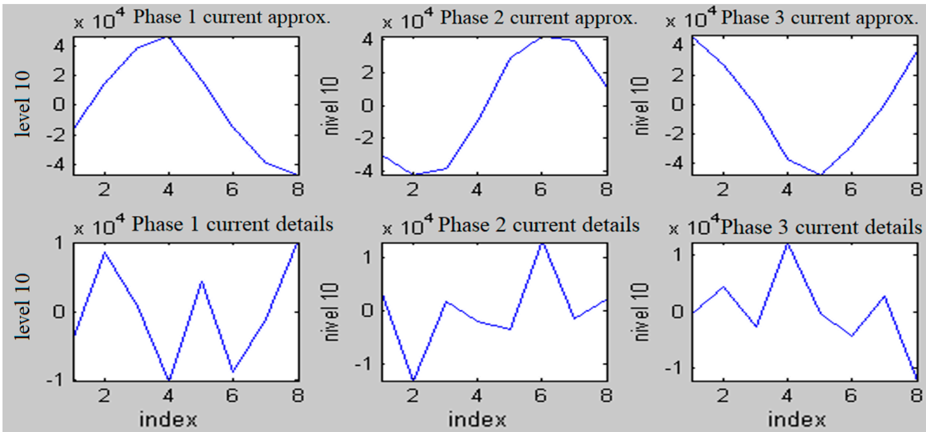

Figure 19. Vectors of approximations and details for current, level 10, first case study.

PQ indices for energy/powers and various categories of powers were computed, making use of the Equations from Section 2.3.1.2 (Equations (111)–(123)) by using original software tools developed by the authors.

Table 2 gathers the most important results yielded by these programs.

Data from Tables 1 and 2 were used to perform a comparison between counterpart PQ indices and powers. Table 3 gathers percentage differences (FFT vs. DWT) relative to FFT between those quantities for which differences were low. Higher differences (up to 20% in absolute value, highest difference being noticed at reactive powers) could be noticed for the rest of the indices. Possible explanations for them are the existence of small differences between half-periods (affecting the accuracy of results yielded by FFT), presence of significant "jumps" in waveforms due to the switch of thyristors, combination of errors with opposite signs at different decomposition methods, inherent errors produced by the use of discrete values and interpolation techniques.

Computations accomplished on synthetic quasi-steady and smooth waveforms revealed a better convergence of results, proving that for those cases, both decomposition techniques and theories can be used to characterize the electric energy quality, to perform a fair charge, to measure and evaluate the load compensation efficiency. For the rest of the cases, DWT provides better results for PQ indices not mentioned in Table 3.

Table 2. Power quality index, powers and power factor computed with DWT and the third theory, first case study.

Parameters	Units	Phase Number		
		1	**2**	**3**
Total RMS of currents	A	1048.01	1054.76	1067.36
RMS of currents for the fundamental harmonic	A	1014.63	1021.28	1030.5
Distorting residues of currents	A	262.42	263.66	278.07
Total harmonic distortions of currents	%	26.04	25.49	26.05
Node zero voltages	V	337.87	336.55	333.59
RMS of voltages for the fundamental harmonic	V	337.2	335.99	332.79
Distorting residues of voltages	V	21.2	19.32	23.09
Total harmonic distortions of voltages	%	6.28	5.74	6.92
Active powers of approximations, *Papp*	kW	99.09	102.55	104.92
Active power of details, *Pdet*	kW	−2.38	−1.91	−2.72
Phase active powers	kW	96.7	100.51	102.2
Total active power of approximations	kW		300.76	
Total active power of details	kW		−7.15	
Total active power	kW		292.98	
Reactive powers of approximations, Q_{app}	kVAr	327.47	327.5	326.51
Reactive powers of details, Q_{det}	kVAr	5.03	4.72	5.82
Total reactive power of approximation	kVAr		985.33	
Distorting powers of currents	kVAd	88.49	88.58	92.54
Distorting powers of voltages	kVAd	21.51	19.73	23.79
Distorting powers of details, D_{det}	kVAd	6.06	5.44	6.97
Non-active powers, N	kVAd	367.06	368.94	370.45
Effective apparent power of approximations S_{app}	kVA	342.14	343.14	342.95
Effective apparent power of details S_{det}	kVA	5.56	5.09	6.42
"Non-approximation" effective apparent power S_{eN}	kVA	91.24	90.9	95.77
Apparent powers	kVA	354.09	354.98	356.07
Effective apparent powers of approximation, S_{eapp}	kVA		1028.31	
Unbalanced power of approximations S_{Uapp}	kVAd		58.84	
Effective apparent powers of details, S_{edet}	kVAd		17.1	
Total distorting power of current, *DeI*	kVA		269.76	
Total distorting power of voltage *DeV*	kVA		65.19	
"Non-approximation" effective apparent power S_{eN}	kVA		278.05	
Total non-active power, N	kVA		1024.15	
Effective apparent powers	kVA		1065.23	
Power factor of approximations on positive sequence			0.291 (inductive character)	
Total power factor			0.275 (with inductive character)	

Table 3. Computed percentage relative differences between power quality indices (FFT vs. DWT)—first case study.

Parameter	Phase Number		
	1	**2**	**3**
Total RMS for currents	0.08	−0.09	0.05
RMS for currents (fundamental harmonic)	−0.31	−0.42	−0.12
Total harmonic distortions of currents	1.58	2.59	2.03
Total RMS for voltages	0.09	0.06	0.06
RMS for voltages (fundamental harmonic)	−0.09	0.05	0.08
Distorting residue of voltages	0.33	3.73	3.96
Total harmonic distortion of voltages	0.32	3.69	4.06
Active powers	0.19	0.23	0.86
Total active power		2.3	
Apparent powers	−0.01	−0.26	0.19
Total apparent power		0.02	
Power factor		2.14	

3.2. Study of Waveforms Acquired from the Primary Winding of a Transformer Used to Supply the Excitation of a Power Group

The second case study is related to the first case study (Figure 2), but now data acquired from the primary winding are analysed. Figure 20 depicts the data acquired data from this test point.

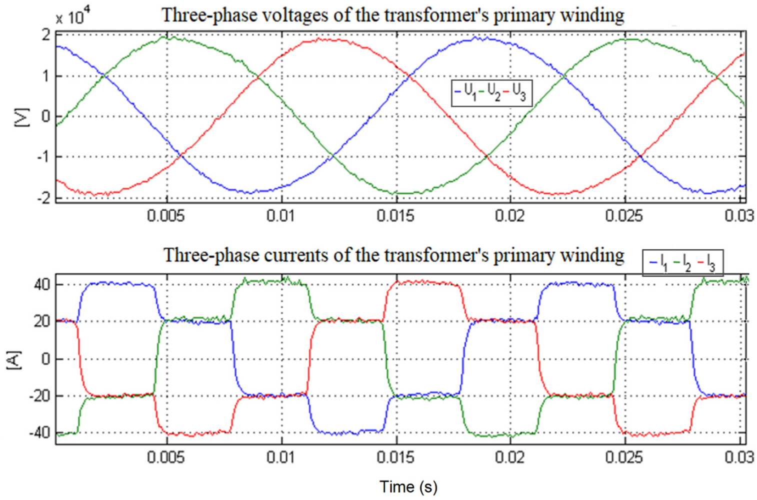

Figure 20. The three-phase voltages and currents acquired in the primary winding of the transformer for the excitation supply.

3.2.1. Data Processing and Powers Computation by Using Fast Fourier Transform

Figure 21 depicts the current and voltage harmonic spectra. Again, only harmonic orders with weights exceeding 1.2% are depicted (therefore, the highest harmonic order displayed in these diagrams is 49).

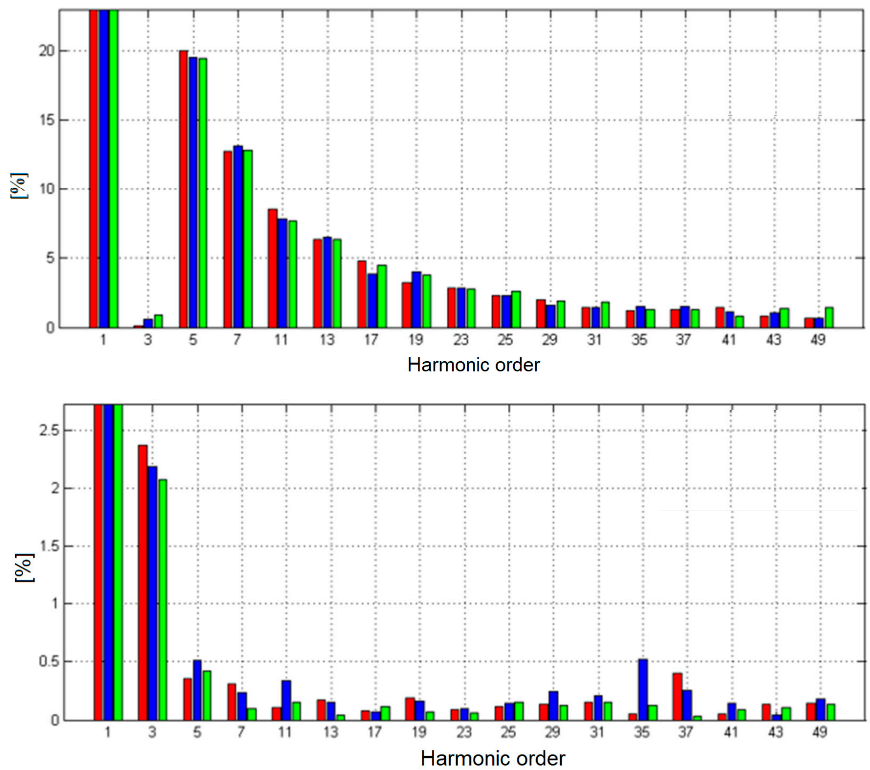

Figure 21. Harmonic spectra of three-phase currents (**top**) and voltages (**bottom**)—acquired at the primary winding of the transformer used for supplying the excitation (harmonic weights > 1.2%).

Similar to the first case study, the spectra of (re)active powers were computed and are depicted in Figure 22.

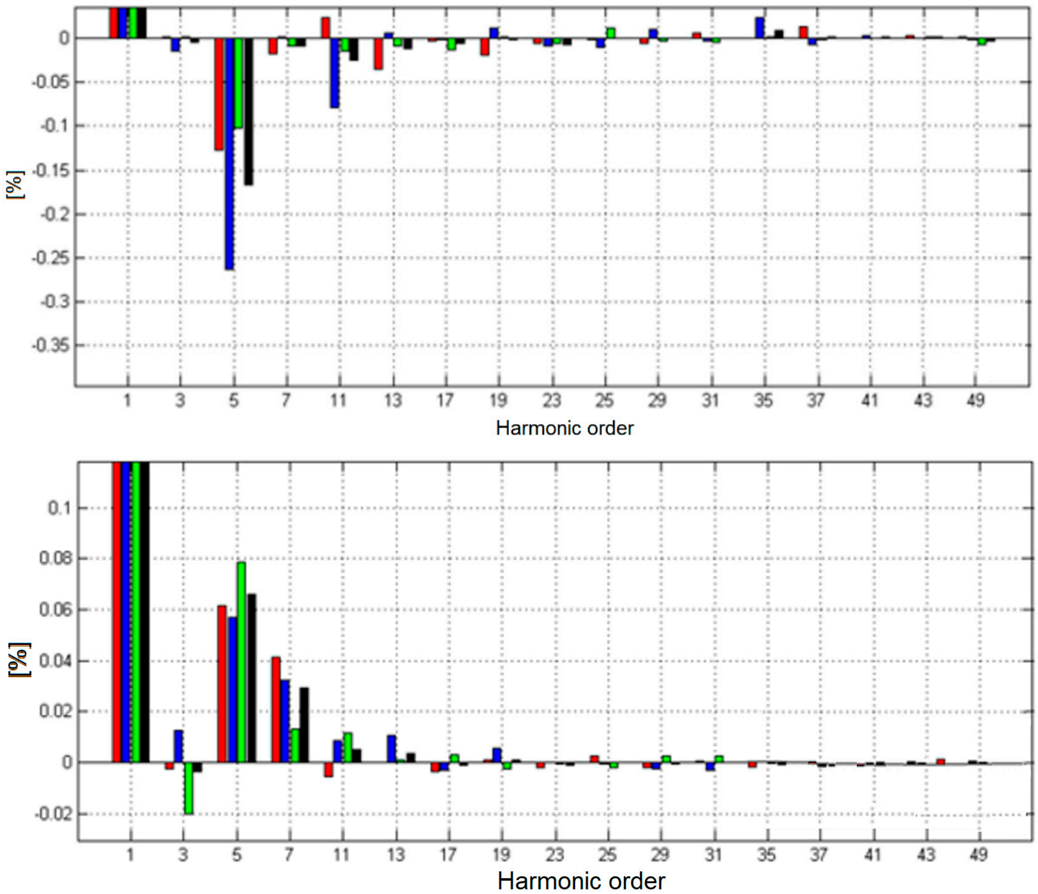

Figure 22. Harmonic spectra of active powers (**top**) and reactive powers (**bottom**)—quantities acquired at the primary winding and secondary winding of the transformer for excitation supply.

Table 4 gathers the results yielded by FFT and the first theory for the second case study.

Remarks:

(a) The low voltage harmonic distortions, in this case, can be explained by the direct connection of the primary winding of T to the national power system. On the other hand, the significant phase current total distortions appear because a fully controlled three-phase rectifier is supplied from SWT. One can notice significant weights of the current harmonic orders from the set {5, 7, 11, 13, 17, 19, 23} and non-negligible harmonic orders from the set {25, 29, 31, 35, 37, 41, 43,49}.

(b) Although the total active power from the primary winding of T was found to be equal to 350.525 kW (very close to the sum of the active powers for the total RMSs along the fundamental harmonic) because the total reactive power was equal to 1064 MVAr (most of it due to the contribution of components associated to the fundamental harmonic) and the total distorting power was equal to 300.92 kVAd (comparable to the active power), the computed value of the power factor was very low (PF = 0.302). This is due to the significant distorting regime from the secondary winding. This regime is transferred in the primary winding of the transformer used for supplying the excitation.

(c) The power flows along the superior harmonics along the superior harmonics are from the primary winding of T toward the power system for the active powers and in the reversed sense for the reactive powers.

(d) A reversed flow of active power along the fundamental harmonic (from the primary toward the secondary winding of T) was also noticed.

(e) The apparent power along the fundamental harmonic (1119.94 MVA) was lower than the total apparent power.

(f) The lower values of the distorting power can be due to a sort of attenuation of the harmonic currents flowing through the primary winding relative to those flowing through the secondary winding.

Table 4. Power quality indices, powers and power factors using FFT and the first theory for the second case study.

Parameters	Units	Phase Number		
		1	**2**	**3**
Total RMS of currents	A	27.92	29.15	29.62
RMS of currents on the fundamental harmonic	A	26.94	28.15	27.65
Distorting residues of currents	A	7.34	7.56	7.40
Total harmonic distortions of currents	%	26.28	25.95	25.86
Total RMS of voltages	kV	13.532	13.535	13.556
RMS of voltages on the fundamental harmonic	kV	13.526	13.529	13.552
Distorting residues of voltages	V	369.46	371.44	327.05
Total harmonic distortion of voltages	%	2.73	2.74	2.41
Active powers	kW	112.97	123.33	114.23
Total active power	kW		350.53	
Active powers on the fundamental harmonic	kW	113.10	123.73	114.42
Total active power on the fundamental harmonic	kW		351.25	
Reactive powers	kVAr	346.73	360.65	357.07
Reactive powers on the fundamental harmonic	kVAr	346.40	360.25	356.75
Total reactive power	kVAr		1064.45	
Distorting powers	kVAd	99.02	101.98	99.92
Total distorting power	kVAd		300.92	
Apparent powers of phases	kVA	377.88	394.56	387.99
Apparent powers on the fundamental harmonic	kVA	364.40	380.90	374.64
Total apparent power	kVA		1119.94	
Power factor on the fundamental harmonic			0.314 (with inductive character)	
Power factor			0.302 (with inductive character)	

3.2.2. Data Processing and Powers Computation by Using Discrete Wavelet Transform

Similar to the first case study, the acquired data depicted in Figure 19 were decomposed with DWT. Based on their values, quality indices for electric energy/power were computed. The most relevant of them for this study are gathered in Table 5.

Similar to the first case study, data from Tables 4 and 5 were used to perform comparisons (FFT vs. DWT) between certain counterpart quantities. Percentage relative differences for some of them are gathered in Table 6.

Table 5. Power quality indices, the powers and power factor using DWT and the third theory, second case study.

Parameters	Units	Phase Number		
		1	2	3
Total RMS of currents	A	27.90	29.17	28.63
RMS of currents on the fundamental harmonic	A	26.95	28.23	27.74
Distorting residues of currents	A	7.19	7.33	7.07
Total harmonic distortions of currents	%	26.95	26.63	26.34
Node zero voltage	kV		13.54	
Total RMS of voltages	kV	13.545	13.527	13.551
RMS of voltages on the fundamental harmonic	kV	13.542	13.52	13.548
Distorting residue of voltages	V	206.34	285.26	235.66
Total harmonic distortion of voltages	%	1.52	2.11	1.74
Active powers of approximations, P_{app}	kW	112.73	125.36	113.84
Active powers of details, P_{det}	W	448.20	−1153.99	−60.60
Active powers	kW	113.18	124.21	113.77
Total active power of approximation	kW		350.67	
Total active power of details	W		−766.39	
Total active power	kW		349.90	
Reactive powers of approximations, Q_{app}	kVAr	347.18	360.57	358.25
Active powers of details, Q_{det}	kVAr	1.414	1.745	1.665
Total reactive power of approximation	MVAr		1.065	
Current distorting powers	kVAd	97.37	99.19	95.80
Voltage distorting powers	kVAd	5.561	8.052	6.538
Distorting powers of details, D_{det}	kVAd	1.549	2.389	1.667
Non-active powers, N	kVAd	394.42	413.60	404.31
Apparent powers of approximations, S_{app}	kVA	365.02	381.74	375.90
Apparent powers of details, S_{det}	kVA	1.483	2.092	1.666
"Non-approximation" apparent power, S_N	kVA	97.54	99.54	96.04
Apparent powers	kVA	377.83	394.50	387.98
Effective apparent powers of approximation, S_{eapp}	MVA		1.123	
Unbalanced power of approximations, S_{Uapp}	kVAd		67.123	
Effective apparent powers of details, S_{edet}	kVAd		5.283	
Total distorting power of current, D_{eI}	kVA		292.396	
Total distorting power of voltage, D_{eV}	kVA		20.287	
"Non-approximation" effective apparent power S_{eN}	kVA		293.146	
Total non-active power, N	MVA		1.107	
Total effective apparent powers	MVA		1.161	
Power factor of approximations on positive sequence			0.313 (with inductive character)	
Total power factor			0.302 (with inductive character)	

Table 6. Computed percentage relative differences between power quality index (FFT vs. DWT) second case study.

Parameters	Phase Number		
	1	2	3
Total RMS of currents	0.071	0.069	3.342
RMS on the fundamental harmonic of currents	0.037	0.284	0.325
Distorting residue of currents	2.043	3.042	4.459
Total harmonic distortion of currents	2.48	2.55	1.82
Total RMS of voltages	0.092	0.062	0.042
Active powers	0.186	0.714	0.402
Total active power		0.180	
Apparent powers	0.014	0.015	0.193
Power factor		0.188	

The analysis of comparison results yielded similar conclusions as those drawn in the first case study.

3.3. Study of Waveforms Acquired from the Terminals of the Main Generator from a Power Group

The third case study approaches almost sinusoidal waveforms (Figure 23), acquired from the terminals of the main generator from a power group that supplies power of around 171 MW to the national power system.

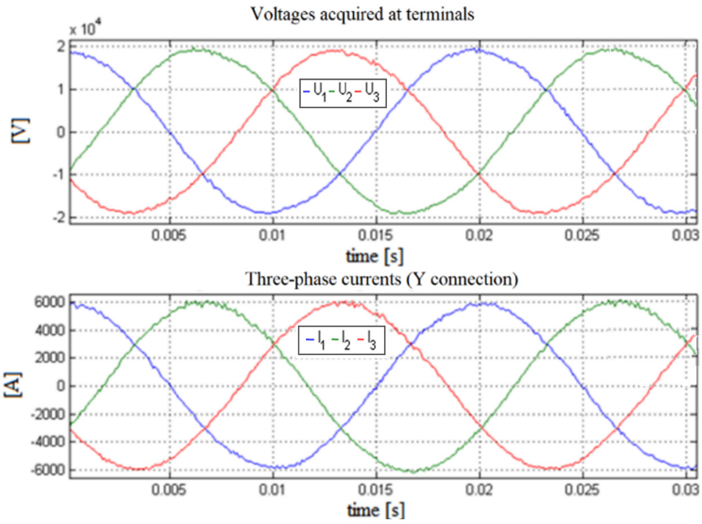

Figure 23. Three-phase voltages and currents acquired from the main generator terminals for an active power of 171 MW delivered to the national power system.

3.3.1. Data Processing and Powers Computation by Using Fast Fourier Transform

Figure 24 depicts the harmonic spectra of currents and voltages yielded by FFT. Due to the almost sinusoidal shapes of the analysed waveforms, a lower threshold (0.6%) was set for the displayed harmonic weights. The spectra for (re)active powers are depicted in Figure 25.

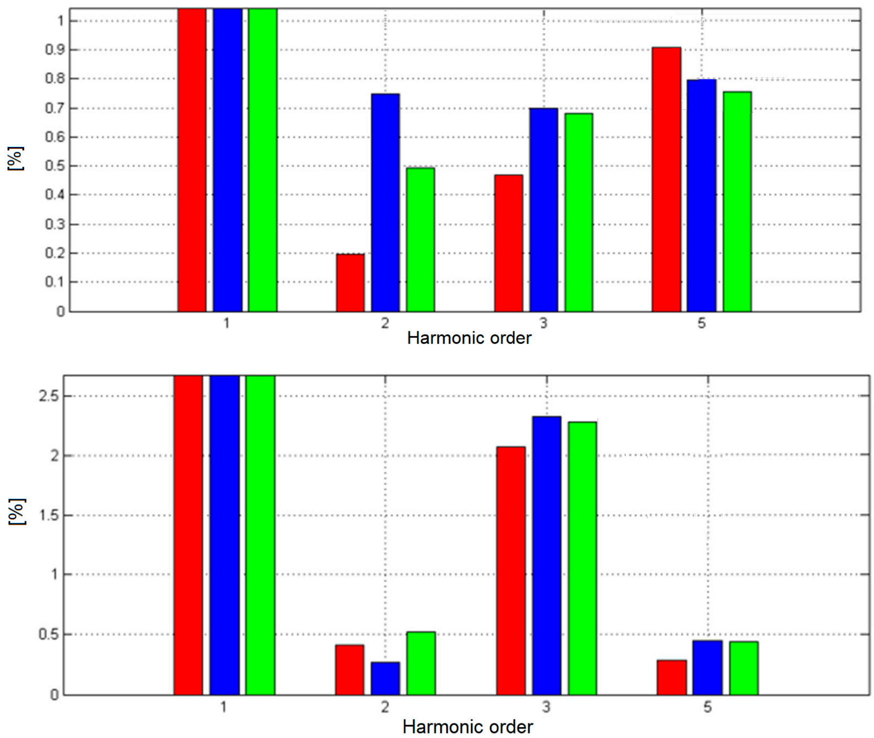

Figure 24. Harmonic spectra of three-phase currents (**top**) and voltages (**bottom**)—quantities acquired at the terminals of the main generator for the active power of 171 MW.

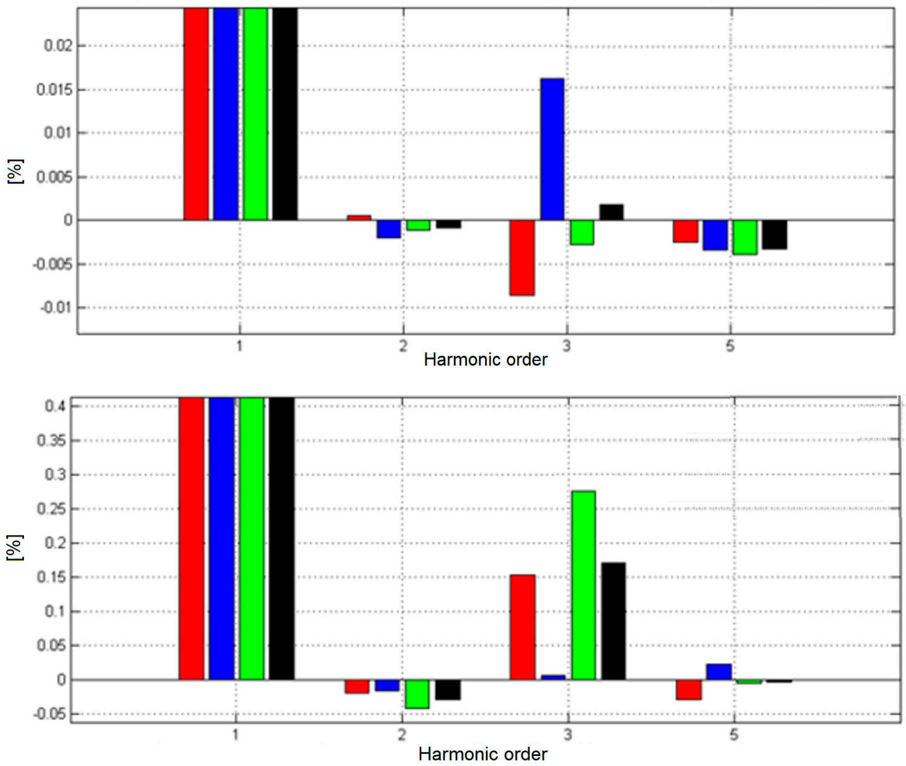

Figure 25. The harmonic spectra of three-phase active powers (**top**) and reactive powers (**bottom**)—quantities acquired at the terminals of the main generator, corresponding to an active power of 171 MW.

Table 7 gathers the results yielded by FFT and the first theory for the third case study.

Table 7. Power quality indices, powers and power factor using FFT and the first theory—third case study.

Parameters	Units	Phase Number		
		1	2	3
Total RMS of currents	A	4125.69	4275.78	4233.23
RMS current of the fundamental harmonic	A	4124.82	4274.77	4232.20
Distorting residue of currents	A	74.38	87.83	93.11
Total harmonic distortion of currents	%	1.80	2.05	2.20
Total RMS of voltages	V	13,613.39	13,591.04	13,539.51
RMS voltage of the fundamental harmonic	V	13,609.05	13,585.98	13,534.1981
Distorting residue of voltages	V	341.64	369.66	375.26
Total harmonic distortion of voltages	%	2.51	2.72	2.77
Active powers	MW	56.10	58.05	57.19
Total active power	MW		171.34	
Active powers on the fundamental harmonic	MW	56.11	58.05	57.19
Total active power on the fundamental harmonic	MW		171.35	
Reactive powers	MVAr	16.62	184.47	319.01
Reactive powers on the fundamental harmonic	MVAr	16.60	18.44	31.82
Total reactive power	MVAr		66.96	
Distorting powers	MVAd	2.05	1.87	2.13
Total distorting power	MVAd		6.05	
Apparent powers	MVA	56.08	57.86	56.53
Apparent powers on the fundamental harmonic	MVA	56.16	58.11	57.32
Total apparent powers	MVA		171.59	
Power factor on the fundamental harmonic			0.999 (inductive character)	
Power factor			0.998 (inductive character)	

1. The reduced harmonic distortions for all waveforms prove that the synchronous generator connected to the national power system was in a safe operating regime. It did not affect and was not affected by the national power system.

2. The total active power was equal to 171.34 MW, a value that is very close to the active power of the fundamental harmonic. The total reactive power was equal to 66.96 MVAr, at its turn, very close to the reactive power of the fundamental harmonic. At the same time, the total distorting power was equal to 6.05 MVAd, whilst the total apparent power had a value of 171.59 MVA. The close values of the total apparent and active powers were reflected by the power factor (PF = 0.998), which was very close to the ideal value of 1. These observations can also be correlated to the reduced values of the computed reactive and distorting powers.

For this case, one could conclude that the consumption of reactive power into the system was small, even if the data were acquired in a moment with the regular operation of the national power system.

The distorting power had a small value, being influenced by the national power system, which introduced a weak non-sinusoidal regime. Therefore, one can consider that the generator operating regime was almost sinusoidal.

3.3.2. Data Processing and Powers Computation by Using Discrete Wavelet Transform

Again, the data for the third case study were decomposed with DWT, considering the same methodology used in the first 2 case studies. The results are gathered in Table 8.

Table 8. Power quality indices, the powers and power factor using DWT and the third theory.

Parameters	Units	Phase Number		
		1	2	3
Total RMS of currents	A	4127.10	4280.16	4267.74
RMS of currents for the fundamental harmonic	A	4126.13	4279.42	4266.13
Distorting residue of currents	A	89.26	79.50	117.10
Total harmonic distortion of currents	%	2.16	1.86	2.74
Node zero voltage	kV		13.621	
Total RMS of voltages	kV	13.617	13,620	13,636
RMS of voltages for the fundamental harmonic	kV	13,614	13.618	13.631
Distorting residue of voltages	V	270.73	213.37	377.76
Total harmonic distortion of voltages	%	1.99	1.57	2.77
Active power of approximations, P_{app}	MW	56.13	58.24	58.04
Active power of details, P_{det}	MW	12.719	14.36	22.652
Phase active powers	MW	56.17	58.28	58.07
Total active power of approximations	kW		171,800	
Total active power of details	kW		36.81	
Total active power	kW		171,837	
Reactive power of approximations, Q_{app}	MVAr	2.37	2.26	3.55
Reactive power of details, Q_{det}	kVAr	20.55	16.9	37.99
Total reactive power of approximation	kVAr		16,912	
Distorting powers of currents	MVAd	1.22	1.08	1.59
Distorting powers of voltages	MVAd	1.12	0.91	1.61
Distorting powers of details D_{det}	kVAd	27.31	17.02	49,69
Non-active powers, N	MVAd	79.44	82.4	82.21
Apparent power of approximations S_{app}	MVA	56.17	58.28	58.15
Apparent power of details S_{det}	kVA	24.16	16.96	44.24
"Non-approximation" apparent power S_{eN}	MVA	1.65	1.42	2.27
Apparent powers	MVA	56.20	58.30	58.20
Effective apparent powers of approximation, S_{eapp}	MVA		172.63	
Unbalanced power of approximation S_{Uapp}	MVAd		20.15	
Effective apparent powers of details, S_{edet}	kVAd		85.57	
Total current distorting power, D_{eI}	MVA		3.95	
Total voltage distorting power D_{eV}	MVA		3.74	
Effective apparent power	MVA		172.71	
Power factor of approximations on positive sequence			0.9952 (inductive character)	
Total power factor			0.9949 (inductive character)	

Side-by-side results, computed with FFT and DWT, are gathered in Table 9.

Table 9. Computed Values of Power Quality indices (FFT vs. DWT).

Parameters	Calculation Method	Phase Number		
		1	2	3
Total RMS of currents [A]	FFT DWT	4125.69 4127.10	4275.78 4280.16	4233.23 4267.74
Total harmonic distortion of currents [%]	FFT DWT	1.80 2.16	2.05 1.86	2.20 2.74
Total RMS of voltages [V]	FFT DWT	13,613.39 13,617	13,591.04 13,620	13,539.51 13,636
Total harmonic distortion of voltages [%]	FFT DWT	2.51 1.99	2.72 1.57	2.77 2.77
Total phase active powers {MW]	FFT DWT	56.10 56.17	58.05 58.28	57.19 58.07
Total active power [MW]	FFT DWT		171.34 171.84	
Total apparent power [MVA]	FFT DWT		171.59 172.71	
Total power factor	FFT DWT		0.9854 0.9949	

Again, one can notice non-significant differences between the compared results. The explanations for differences were presented in the first case study.

The company operating this electric power generator could correctly handle the power balance as long as accurate data were provided by performing data acquisition systems; software tools based on FFT and DWT, implementing correct theories, were used. The correct measurement of the energies/powers delivered to the national power system made possible the establishment of a correct charge for the delivered energy/power.

4. Conclusions

The theories dealing with powers in non-sinusoidal and non-symmetrical regimes should be able to allow for a correct evaluation of powers, appropriate test possibilities, modalities for the compensation of unpleasant effects, as well as for correct quantification of the measures used to diminish these effects through compensation. Such theories, able to satisfy at least partially these requirements, are approached in this paper, but not all theories issued until now can do this.

Most of the theories for non-sinusoidal regimes rely on the Fourier Transform. Usually, the people authoring definitions make use of harmonic decompositions, but alternative definitions coexist as well (also using to an end the Fourier Transform [27–31]). Based on these theories, one can evaluate indices of quality for waveforms (e.g., [32,33]), and powers, respectively. However, the decomposition in harmonic components is limited to the highest harmonic orders to be considered by the actual standards [6,7]. Therefore, one can deal only with problems related to the quality of powers/energies and cannot address problems related to electromagnetic interferences specific to the domain of Electromagnetic Compatibility.

One has to underline that it is more difficult to evaluate the non-symmetries occurring in three-phase systems in terms of the Fourier series. There are different sequences for different harmonic orders (e.g., at currents: "+" for harmonic orders 3*m + 1, "−" for harmonic orders 3*m + 2, "0"—for harmonic orders 3*m), and moreover, it is possible to have a cross-power between different sequences quite along the fundamental harmonic (17), proving that these components of different sequences have to be discussed along with the harmonics related to Fourier series. Neither the separation of unbalanced harmonic components in the Standard IEEE 1459-2010 might represent a solution as long as those harmonic components (which actually are non-symmetrical instead of unbalanced!) are yielded by the decomposition using Fourier series for non-sinusoidal regimes. Such components appear in both the second and third theories approached in this paper, denoting no special relevance from a practical point of view.

A fourth theory, based on the definitions of certain instantaneous real and imaginary powers, is useful for active or hybrid dynamic compensation processes (as mentioned in [34–37]), but it cannot be considered as a standalone theory of powers as long as it does not fulfil all the requirements. Therefore, to justify the compensation efficiency, one has to use one of the other theories. Maybe the correct name of this theory will be: **"The compensation based on the definition using the real and imaginary powers definition"** (not as a theory for powers in a three-phase system).

Three examples of real data processing are presented for the first and third theories. Data corresponding to voltages and currents waveforms were acquired with DASs specially designed for these applications. Dedicated software tools relying on Fast Fourier Transform and Discrete Wavelet Transform were conceived. The topology of the DWT tree used for decomposition can be characterized as follows: 8192 components in the root node, 10 levels and a wavelet mother from the Daubechies family with a filter consisting of 8 components. The quantities defined in the approached theories were computed and comparisons of those who can be considered as analogue were made such as to prove the correctness of the evaluation of power definitions, PQ indices and power factors.

The first case study is concerned with the analysis of data acquired from the secondary winding of a transformer used to supply the excitation of a power group. In the work frame of the first theory, one computed (re)active, distorting and apparent powers in a correct approach because they provide information that is useful for the compensation modalities as well. This theory meets the requirements relative to its usefulness. Computations were made considering the third theory as long as it defines the same quantities as the second one (from the IEEE Standard 1459-2010). Harmonic orders higher than the limits imposed by the standard are considered too by the software tools, providing more accurate results. The comparison accomplished between the computed results for the analogue quantities was made using tables and percentage differences relative to the results yielded by FFT and revealed small differences. In this case, both three-phase voltages and currents have non-sinusoidal shapes. This is also revealed by the analysis of the THD values.

The second case study is concerned with the analysis of data acquired from the primary winding of the same transformer used to supply the excitation of a power group addressed by the first case study. Considering the same methodology as the one applied for the first case, small differences were revealed again between the numerical results yielded within the work frame of the compared theories for analogue quantities. The analysis of data for the first two case studies revealed significant non-sinusoidal regimes. Significant distortions were noticed in both voltages and currents acquired from the secondary winding of the transformer used to supply the excitation, unlike the case of the primary winding of the same transformer. This happens because high voltages characterize the second case study, which is not influenced by the currents flowing through the transformer. Therefore, the harmonic currents produced in the secondary winding are transmitted to the primary winding but have no influence over the three-phase voltages from it. The powers measured in the primary winding are higher than those from the secondary winding due to the losses from the transformer (both along the fundamental and superior harmonics). In this case, the non-sinusoidal shapes are noticed only at the three-phase currents. This characteristic is also revealed by the analysis of THDs for voltages and currents. Independent DASs were used for the first two cases approached in this paper. Yet they can operate jointly using a synchronization provided by an original software tool.

The third example refers to an almost sinusoidal regime in which certain components of powers (reactive, apparent, non-active etc.) are small. In this case, too, it is proved that one can apply any of the first and third theories to obtain correct results of measurement and charge for consumers. The differences noticed between the results yielded by FFT and DWT can be explained by the existence of small differences between half-periods (affecting the accuracy of results yielded by FFT), presence of significant "jumps" in waveforms due to the switch of thyristors (for the first two case studies), a combination of errors with opposite signs at different decomposition methods and inherent errors produced by the use of discrete values and interpolation techniques. In this case, all waveforms are almost sinusoidal, a fact that is also revealed by the analysis of the THDs.

The examples from Section 3 reveal that the first and third theories can be used for an accurate evaluation of powers and power factors. Appropriate software tools developed by authors, relying on FFT and, respectively, DWT, implement these theories and yield reliable results. When the implementation of DWT is unavailable, one can use the first two theories and employ FFT (considering its usability limits).

The numerical processing allowed for a correct diagnosis of the synchronous generator excitation winding, whose schematic is depicted in Figure 2. The compensation solution deduced by the authors based on the results of the numerical processing relies on the joint utilization of an active filter, along with reactance coils. This solution requires the application of the fourth theory and is currently during the implementation stage. The solution validation will make use of the first and third theories to perform an evaluation from both technical and economic points of view.

The third example reveals a correct determination of the power/energy delivered by a synchronous generator G2 to the power system. G2 belongs to a power group PG2 other than that approached in the first two cases (PG1). The implementation of this solution at PG2 determined its technical staff to give up the analogue apparatus and rely on the solution proposed by the authors for a correct test and management of the electric power/energy.

In a general conclusion, one can say that the theories approached in this paper fulfil the requirements for which they were created, except for the fourth theory, which can meet only the requirements related to compensation scopes and cannot provide a correct methodology for the correct measurement of powers or power factors.

Author Contributions: Conceptualization, P.-M.N.; methodology, P.-M.N. and M.-Ş.N.; software, I.-D.N.; validation, I.-D.N. and M.-Ş.N.; investigation, P.-M.N. and M.-Ş.N.; data curation, P.-M.N., M.-Ş.N. and I.-D.N.; writing—original draft preparation, P.-M.N.; writing—review and editing, I.-D.N.; visualization, supervision, P.-M.N. All authors have read and agreed to the published version of the manuscript.

Funding: This research received no external funding.

Data Availability Statement: Not applicable.

Conflicts of Interest: The authors declare no conflict of interest.

Nomenclature

$u_1(t),\ u_2(t),\ u_3(t)$	instantaneous three-phase voltages
U_k	the voltage RMS value for the k'th order harmonic
γ_k	initial phase for the k-th order harmonic voltage
$i_1(t),\ i_2(t),\ i_3(t)$	instantaneous three-phase currents
I_k	the current RMS value for the k'th order harmonic
θ_k	initial phase for the k-th order harmonic current
$U_1,\ U_2,\ U_3$	the vectors (first-order tensors) of the phase voltages in the vectorial space E, in Antoniu–Gafencu Theory
I_1, I_2, I_3	the vectors (first-order tensors) of the phase currents in the vectorial space E, in Antoniu–Gafencu Theory

$K_x \cdot U_k \cdot cos\gamma_k$, $K_x \cdot U_k \cdot cos\left(\gamma_k - k \cdot \frac{2\pi}{3}\right)$, $K_x \cdot U_k \cdot cos\left(\gamma_k + k \cdot \frac{2\pi}{3}\right)$	the projections of the vectors U_1, U_2, U_3 along the axis Kx of a subspace E1 of odd functions (similar equations can be written for currents);
$K_y \cdot U_k \cdot cos\gamma_k$, $K_y \cdot U_k \cdot cos\left(\gamma_k - k \cdot \frac{2\pi}{3}\right)$, $K_y \cdot U_k \cdot cos\left(\gamma_k + k \cdot \frac{2\pi}{3}\right)$	the projections of the vectors U_1, U_2, U_3 along the axis Ky of a subspace E2 of odd functions (similar equations can be written for currents).
$\varphi_k = \gamma_k - \theta_k$	phase-shift between the voltage and the current corresponding to the harmonic order k, in the Antoniu–Gafencu Theory
$\varphi_l = \gamma_l - \theta_l$	phase-shift between the voltage and the current corresponding to the harmonic order l, in the Antoniu–Gafencu Theory
P	total active power of the (un)balanced three-phase network operating in a distorting regime
P_1, P_2, P_3	active powers for each of the three phases in the Antoniu–Gafencu Theory
$\beta = e^{j\frac{\pi}{2}} = cos\frac{\pi}{2} + j \cdot sin\frac{\pi}{2} = j$	rotation operator with $\frac{\pi}{2}$
$\Lambda = \beta = e^{-j\frac{\pi}{2}} = cos\left(-\frac{\pi}{2}\right) + j \cdot sin\left(-\frac{\pi}{2}\right) = -j$	rotation operator with $\left(-\frac{\pi}{2}\right)$
Q	total reactive power, in the Antoniu–Gafencu Theory
D	total distorting power in the Antoniu–Gafencu Theory
D_1, D_2, D_3	distorting power for each phase in the Antoniu–Gafencu Theory
V_0, V_+, V_-	zero-sequence, positive-sequence, negative-sequence components of phase voltages
U_{+_k}	positive sequence voltage for the kth harmonic order in the Antoniu–Gafencu Theory
U_{-_k}	negative sequence voltage for the kth harmonic order
U_0	zero sequence voltage for the kth harmonic order
I_{+1}, I_{+2}, I_{+3}	positive sequence current components of phases in the Antoniu–Gafencu Theory
I_{+_k}	positive sequence current for the kth harmonic order
I_{-1}, I_{-2}, I_{-3}	negative sequence current components of phases in the Antoniu–Gafencu Theory
I_{-_k}	negative sequence current for the kth harmonic order in the Antoniu–Gafencu Theory
I_{01}, I_{02}, I_{03}	zero sequence current components of phases in the Antoniu–Gafencu Theory
I_{0_k}	zero sequence current for the kth harmonic order in the Antoniu–Gafencu Theory
I_e	total Root Mean Square (RMS) current in IEEE 1459 Std.
I_{e1}	RMS current of the fundamental harmonic in IEEE 1459 Std.
I_{eH}	equivalent RMS harmonic current in IEEE 1459 Std.
V_e	total Root Mean Square (RMS) voltage in IEEE 1459 Std.
V_{e1}	RMS voltage of the fundamental harmonic in IEEE 1459 Std.
V_{eH}	equivalent RMS harmonic voltage in IEEE 1459 Std.
S_e	total effective apparent power in IEEE 1459 Std.
S_{e1}	fundamental effective apparent power in IEEE 1459 Std.
S_{U1}	non-symmetrical apparent power in IEEE 1459 Std.
$S^+{}_1$	fundamental positive-sequence apparent power in IEEE 1459 Std.
S_{eN}	nonfundamental effective apparent power in IEEE 1459 Std.
DeI	current distortion power in IEEE 1459 Std.
D_{eV}	voltage distortion power in IEEE 1459 Std.
S_{eH}	harmonic apparent power for superior harmonics in IEEE 1459 Std.
P_{eH}	harmonic active power for superior harmonics in IEEE 1459 Std.
D_{eH}	harmonic distortion power for superior harmonics in IEEE 1459 Std.
THD_{eV}	equivalent total voltage harmonic distortion in IEEE 1459 Std.
THD_{eI}	equivalent total current harmonic distortion in IEEE 1459 Std.
$P^+{}_1$	fundamental positive-sequence active power in IEEE 1459 Std.
$Q^+{}_1$	fundamental positive-sequence reactive power in IEEE 1459 Std.
PF_1^+	fundamental positive-sequence power factor in IEEE 1459 Std.
PF_e	equivalent power factor in IEEE 1459 Std.
$PF^+{}_1$	fundamental positive-sequence power factor in IEEE 1459 Std.
$c'_{j0,k}$	discrete wavelet coefficient corresponding to the voltage for the level j_0
$d'_{j,k}, d_{j,k}$	discrete Wavelet coefficients for the levels $j \neq j_0$, sample k
V_{j_0}	RMS voltage value for the level with the lowest frequency j_0 ("approximation" voltage)
V_j	RMS voltage for higher frequency bands ("details" voltage)

$c_{j0,k}$	discrete Wavelet coefficient corresponding to the current for the level j_0
I_{j_0}	RMS current value for the level with the lowest frequency j_0 ("approximation" current)
I_j	RMS current for higher frequency bands ("details" current)
$\psi_{j,k}$	Wavelet function
P_{app}	single-phase approximation active power in the Morsi theory
P_{det}	single-phase details active power in the Morsi theory
P_j	single-phase active power for higher frequency bands ("details" active power)
N	single-phase non-active power in the Morsi theory
S_{app}	single-phase approximate apparent power in the Morsi theory
V_{det}	single-phase RMS voltage for higher frequency bands ("details" voltage)
I_{det}	single-phase RMS current for higher frequency bands ("details" current)
S_N	single-phase "non-approximation" apparent power
dPF	single-phase displacement power factor (dPF)
PF	single-phase total power factor
PF_{osc}	single-phase oscillating power factor
DP	single-phase details pollution
V_{eapp}, I_{eapp}	"approximation" effective RMS values for three-phase voltages and currents in the Morsi theory
V_{det}, I_{det}	"details" effective RMS values for three-phase voltages and currents in the Morsi theory
V_e, I_e	three-phase effective RMS values of voltage and current in the Morsi theory
P^+_{app}	three-phase positive sequence active power in the Morsi theory
P	total active power in the Morsi theory
S_{eapp}	three-phase "approximation" effective apparent power in the Morsi theory
S_{Uapp}	three-phase "approximation" unbalanced power in the Morsi theory
$S^+{}_{app}$	three-phase positive sequence apparent approximation power in the Morsi theory
$V^+{}_{app}$, $I^+{}_{app}$	positive sequence effective RMS approximation voltage, current in the three-phase case in the Morsi theory
S_{eN}	three-phase "non-approximation" effective apparent power in the Morsi theory
S_{edet}	three-phase details apparent power in the Morsi theory
$PF^+{}_{app}$	three-phase "approximation" positive sequence power factor in the Morsi theory
LU	load unbalance in the Morsi theory
p	instantaneous power in the Akagi theory
$\alpha\beta 0$	the stationary reference frame used in the Akagi theory for the Clarke transformation
$u_a(t)$, $u_b(t)$, $u_c(t)$	phase voltages of a three-phase load in the Akagi theory
$i_a(t)$, $i_b(t)$, $i_c(t)$	phase currents of a three-phase load in the Akagi theory
$u_\alpha(t)$, $u_\beta(t)$, $u_0(t)$	modified α, β, 0 voltage components supplying the load in the Akagi theory
$i_a(t)$, $i_\beta(t)$, $i_0(t)$	modified α, β, 0 current components supplying the load in the Akagi theory
$p_a(t)$, $p_b(t)$, $p_c(t)$	phase active powers
$p_\alpha(t)$, $p_\beta(t)$	the instantaneous real power without zero-components in the Akagi theory
$p_r(t)$	total instantaneous real power without zero-components in the Akagi theory
$p_0(t)$	the instantaneous zero power in the Akagi theory
$p_i(t) = q(t)$	instantaneous imaginary (reactive) power in the Akagi theory
$\overline{p}, \widetilde{p}(t)$	average and fluctuating components of the instantaneous real power $p_r(t)$
$\overline{q}, \widetilde{q}(t)$	average and fluctuating components of the instantaneous reactive power $p_i(t)$

References

1. Budeanu, C. *Puissances Reactives and Fictives*; Institut National Roumaine–pour l'etude de l'amenagement et de l'utilisation des Sources de l'energie: Bucharest, Romania, 1927.
2. Fryze, S. Wirk-, Blind- und Scheinleistung in Electrisken Stromkreisen mit nichtsinusoidalen, Verlauf von Strom und Spannung. *ETZ* **1931**, *25*, 33.
3. Depenbrock, M. *Wirk-und Blindleistung*; ETG-Fachtagung "Blindleistung": Aachen, Germany, 1979.
4. Kusters, N.L.; Moore, W.J.M. On the definition of reactive power under nonsinusoidal conditions. *IEEE Trans. Power Appl. Syst.* **1980**, *PAS-99*, 1845–1854. [CrossRef]
5. Czarnesky, L.S. Powers in nonsinusoidal networks, interpretation and measurement. *IEEE Trans. Instrum. Meas.* **1990**, *39*, 340–345. [CrossRef]
6. Depenbrock, M. The FDB-method a generalized applicable tool for analyzing power relations. *IEEE Trans. Power Deliv.* **1993**, *8*, 381–387. [CrossRef]
7. *European Standard EN 50160*; Voltage Characteristics of Electricity Supplied by Public Distribution Systems. CENELEC: Brussels, Belgium, 1999.

8. *IEEE Standard 519-2014*; IEEE Recommended Practice and Requirements for Harmonic Control in Electric Power Systems. IEEE: Piscataway, NJ, USA, 2014.
9. Czarnesky, L.S. Currents' Physical Components (CPC) concept: A fundamental of power theory. In Proceedings of the 2008 International School on Nonsinusoidal Currents and Compensation (ISNCC), Zielona Gora, Poland, 10–13 June 2008; pp. 727–732. [CrossRef]
10. Czarnecki, L.S.; Haley, P. Reactive compensation in three-phase four-wire systems at sinusoidal voltages and currents. In Proceedings of the International School on Nonsinusoidal Currents and Compensation 2013 (ISNCC 2013), Zielona Gora, Poland, 17–20 June 2012; pp. 727–732. [CrossRef]
11. Akagi, H.; Kanazawa, Y.; Nabae, A. Generalized theory of the instantaneous reactive power in three-phase circuits. In Proceedings of the International Power Electronics Conference—IPEC'83, Tokyo, Japan, 27–31 March 1983; pp. 1375–1386.
12. Akagi, H.; Ogasawara, S.; Kim, H. The theory of instantaneous power in three-phase four-wire systems: A comprehensive approach. In Proceedings of the Conference Record of the 1999 IEEE Industry Applications Conference, Thirty-Forth IAS Annual Meeting (Cat. No. 99CH36370), Phoenix, AZ, USA, 3–7 October 1999; IEEE: Piscataway, NJ, USA, 1999; Volume 1, pp. 431–439. [CrossRef]
13. Akagi, H.; Kanazawa, Y.; Nabae, A. Instantaneous Reactive Power compensators comprising switching devices without energy storage components. *IEEE Trans. Ind. Appl.* **1984**, *IA-20*, 625–630. [CrossRef]
14. Antoniu, I.S.; Gafencu, M. Les puissances dans une systeme triphase fonctionnant en regime deformant. *Rev. Roum. Des Sci. Tech. (RRST) Electroteh. Energetique* **1976**, *21*, 519–530.
15. Antoniu, I.S.; Gafencu, M. L'expresion des puissance dans une systeme triphase desequilibre et deformant en fonction des composantes symetrique. *Rev. Roum. Des Sci. Tech. (RRST) Electroteh. Energetique* **1977**, *22*, 3–10.
16. *IEEE 1459-2010*; Definitions for the Measurement of Electric Power Quantities under Sinusoidal, Nonsinusoidal, Balanced, or Unbalanced Conditions Unbalanced and Nonlinear Systems. IEEE: Piscataway, NJ, USA, 2010.
17. Nicolae, P.M. Considerations on instantaneous components of powers based on the decomposition of voltages and currents in instantaneous symmetrical components. In *Proceedings of the 3rd National Seminar for theoretical Electrotechnics, Al Treilea Seminar National de Electrotehnica Teoretica*; Politechnica University Bucuresti: Bucharest, Romania, 1997; pp. 1–12.
18. Morsi, W.G.; El-Hawary, M.E. Reformulating Power Components Definitions Contained in the IEEE Standard 1459-2000 Using Discrete Wavelet Transform. *IEEE Trans. Power Deliv.* **2007**, *22*, 1910–1916. [CrossRef]
19. Morsi, W.G.; El-Hawary, M.E. Reformulating Three-Phase Power Components Definitions Contained in the IEEE Standard 1459-2000 Using Discrete Wavelet Transform. *IEEE Trans. Power Deliv.* **2007**, *22*, 1917–1923. [CrossRef]
20. Nicolae, I.D.; Nicolae, P.M. Using Wavelet Transform for the Evaluation of Power Quality in Distorting Regimes. *Acta Electroteh.* **2011**, *52*, 445–448.
21. Nicolae, I.D.; Nicolae, P.M.; Purcaru, D.M. Computational Issues Related to the Discrete Wavelet Analysis of Power. *Ann. Univ. Craiova Autom. Comput. Electron. Mechatron. Ser.* **2011**, *8*, 25–30.
22. Nicolae, I.D.; Nicolae, P.M. Using Discrete Wavelet Transform to evaluate power quality at highly distorted three-phase systems. In Proceedings of the 11th International Conference on Electrical Power Quality and Utilisation, Lisbon, Portugal, 17–19 October 2011. [CrossRef]
23. Nicolae, P.M. On Real and Imaginary Instantaneous Powers Theory in Three-Phase Networks. *Rev. Roum. Des Sci. Tech. (RRST) Ser. Electroteh. Energetique (EEA)* **1995**, *40*, 215–226.
24. Nicolae, P.M. Instantaneous Real and Imaginary Powers at Three-Phase Networks with Balanced Loads that Function Under Distorting Regime. *Rev. Roum. Des Sci. Tech. (RRST) Ser. Electroteh. Energetique (EEA)* **1995**, *40*, 311–319.
25. Bojoi, R.I.; Griva, G.; Bostan, V.; Guerriero, M.; Farina, F.; Profumo, F. Current control strategy for power conditioners using sinusoidal signal integrators in synchronous reference frame. *IEEE Trans. Power Electron.* **2005**, *20*, 1402–1412. [CrossRef]
26. Nicolae, P.M.; Vladut, G.C.; Constantinescu, M.C.; Nicolae, I.D.; Nicolae, M.S.; Constantinescu, I.I. System and Method for Determining Simultaneous of Electrical Measurement from Stations, Substations and Transformer Stations. Patent 127575, 30 December 2016. Awarded with Gold Medal at Geneva International Exhibition of Inventions, 2016.
27. Pigazo, A.; Moreno, V.M. Accurate and computationally efficient implementation of the IEEE 1459-2000 standard in three-phase three-wire power systems. *IEEE Trans. Power Deliv.* **2007**, *22*, 752–757. [CrossRef]
28. Zheng, T.; Makram, E.B.; Girgis, A.A. Evaluating power system unbalance in the presence of harmonic distortion. *IEEE Trans. Power Deliv.* **2003**, *18*, 393–397. [CrossRef]
29. Ferrero, A. Definitions of Electrical Quantities Commonly Used in Non- Sinusoidal Conditions. *Eur. Trans. Electr. Power Eng. (ETEP)* **1998**, *4*, 235–240. [CrossRef]
30. Tenti, P.; Matavelli, P. A Time-Domain Approach to Power Term Definitions under Non-Sinusoidal Conditions. In Proceedings of the Sixth International Workshop on Power Definitions and Measurements under Non-Sinusoidal Conditions, Milano, Italy, 13–15 October 2003; pp. 1–10.
31. Willems, L. Reflections on apparent power and power factor in non-sinusoidal and poly-phase situations. *IEEE Trans. Power Deliv.* **2004**, *19*, 835–840. [CrossRef]
32. Tugulea, A. Criteria for the Definitions of the Electric Power Quality and its Measurement Systems. *Eur. Trans. Electr. Power Eng. (ETEP)* **1996**, *6*, 357–363. [CrossRef]

33. Morsi, W.G.; El-Hawary, M.E. Wavelet Packet Transform-Based Power Quality Indices for Balanced ad Unbalanced Three-Phase Systems under Stationary and Non-stationary Operating Conditions. *IEEE Trans. Power Deliv.* **2009**, *24*, 2300–2310. [CrossRef]
34. Czarnecki, L. Instantaneous Reactive Power p-q Theory and Power Properties of Three-Phase Systems. *IEEE Trans. Power Deliv.* **2006**, *21*, 362–367. [CrossRef]
35. Akagi, H. Modern active filters and traditional passive filters. *Bull. Pol. Acad. Sci. Tech. Ser.* **2006**, *54*, 255–268.
36. Kulvitit, Y. DC analysis of converters using rectifier control cell. In Proceedings of the IEEE International Conference on Industrial Technology—ICIT 2002, Bankok, Thailand, 11–14 December 2002; Volume 2, pp. 774–779. [CrossRef]
37. Stankovic, A.V.; Chen, K. A New Control Method for Input-Output Harmonic Elimination of the PWM Boost-Type Rectifier under Extreme Unbalanced Operating Conditions. *IEEE Trans. Ind. Electron.* **2009**, *56*, 2420–2430. [CrossRef]